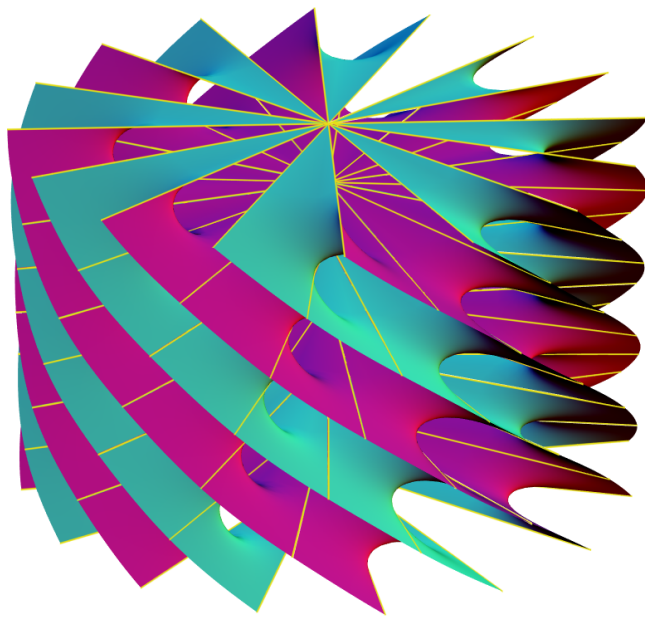# Classical Minimal Surfaces in Euclidean Space by Examples

Geometric and Computational Aspects of the Weierstraß representation

September 25, 2001

Matthias Weber

Contents

1 Introduction

These notes are an enriched version of the lecture notes I distributed for the participants of the Clay Mathmatical Summer School at MSRI, Berkeley, in the summer 2001.

The purpose of the five lectures covered by these notes was to introduce beginning graduate students to minimal surfaces so that they would understand the close interaction between the surface geometry and their complex analytic description.

To achieve this in a fully satisfactory way, I would have needed many prerequisites from differential geometry, partial differential equations, complex variables, Riemann surfaces and topology.

As I was not allowed to assume all this, I have chosen an informal and concrete way to present the subject. Instead of proving theorems, I construct examples, and the more complicated ones only numerically.

The workshop was accompanied by computer sessions where I used my Mathematica notebooks and Jim Hoffman's MESH program to illustrate the examples. The Mathematica notebooks are available on the web.

However, they make use of an add-on to Mathematica, which is not available anymore, the OpenGL explorer. I have been promised that Mathematica 5 will supply the same functionality, and then an updated version of the notebooks will be made available as well.

Thge following sources of further reading ([DHKW92, HK97, Kar89, Oss86]) also indicate where I have borrowed from. I hope that these notes make the articles from the above list more accessible.

Bloomington, September 2001

Matthias Weber

2 Basic Differential Geometry Of Surfaces

We review basic facts about surfaces in euclidean space. Any textbook on elementary differential geometry will do as a reference.

2.1 Local Surface Parameterizations

Denote the standard scalar product of the euclidean space $\mathbb{R}^3$ by $\langle \cdot, \cdot \rangle$. A surface in euclidean space is given by a smooth map from a parameter domain Ω

$$\phi : \Omega \to \mathbb{R}^3$$

We require the map to be non-singular. This means that the differential $d\phi$ has maximal rank 2. Associated to such a surface parameterization are various data which are intended to describe geometric quantities on the surface. Of course, the most interesting data (like curvatures) will be independent of the parameterization. In such a case, it is best to imagine these data as being attached to the surface in $\mathbb{R}^3$ but to compute with these data by representing them in the domain Ω of the surface.

Definition 2.1 *The first fundamental form or Riemannian metric is defined by*

$$g(V, W) = \langle d\phi \cdot V, d\phi \cdot W \rangle$$

It can be used to measure angles and length of tangent vectors. For instance, we can define the length of a curve on a surface by

Definition 2.2 *Let $c : [a, b] \to \Omega$ be a smooth curve. Then the length of $\tilde{c} = \phi \circ c$ is*

$$\text{length}(\tilde{c}) = \int_a^b g(c'(t), c'(t))^{\frac{1}{2}} dt$$

Using the length of curves on the surface, one can define an intrinsic metric (in the usual sense) by declaring the distance between two points as the infimum of the lengths of curves on the surface connecting these two points. There is a useful criteria when a surface, equipped with this metric, is complete. We use this criteria as a definition:

Definition 2.3 *A parameterized surface $\phi : \Omega \to \mathbb{R}^3$ is complete if and only if every smooth curve $c : [0, \infty) \to \omega$ with $c(t) \to \partial\Omega$ for $t \to \infty$ has infinite length on Σ.*

We will mainly be concerned with complete surfaces.

Of particular importance to us is the following special kind of parameterization:

Definition 2.4 *A parameterization is* conformal *or* isothermal *if it preserves the angles between tangent vectors:*

$$\langle d\phi \cdot V, d\phi \cdot W \rangle = \lambda^2 \langle V, W \rangle$$

We call the factor λ the stretch factor *of ϕ.*

In other words, the Riemannian metric is pointwise proportional to the euclidean scalar product of the domain Ω.

If one draws a surface by mapping a square grid to space using an isothermal parameterization, the image quadrilaterals will be close to squares. This makes conformal parameterizations attractive for visualizing surfaces.

2.2 The Stereographic Projection

An important example of a conformal parameterization is the inverse of the stereographic projection. Recall that the stereographic projection maps the unit sphere to the (extended) complex plane. It can be defined as follows: Take a sphere and a plane in $\mathbb{R}^3$. Choose a point P on the sphere but not on the plane. Now, for any point $Q \neq P$ on the sphere there is a straight line l through P and Q, This line intersects the plane in some point Q' — if the line happens to be parallel to the plane, we call the image point the infinite point ∞. The map $Q \mapsto Q'$ is the stereographic projection. It is one-to-one, as for every point Q' in the plane, the line through P and Q' will intersect the sphere in a second point Q.

There are different formulas for this map, depending on the various choices we made. We will use the following formula for the inverse of the stereographic projection. It maps the $z = x + iy$-plane onto the unit sphere in $\mathbb{R}^3$. In complex coordinates,

$$\sigma^{-1}(z) = \left(\frac{2\,\mathrm{Re}(z)}{1 + |z|^2}, \frac{2\,\mathrm{Im}(z)}{1 + |z|^2}, 1 - \frac{2}{1 + |z|^2} \right) \qquad (1)$$

This choice of a stereographic projection maps the north pole (resp. south pole) to ∞ (resp. 0) and the equator to the unit circle.
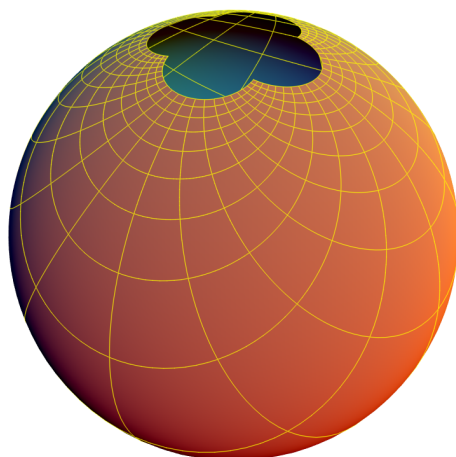
Figure 1: Image of a square grid in the plane under the inverse stereographic projection

Mathematica Notebook **2.1** There is a notebook *Stereographic.nb* which teaches you to use Mathematica to compute the differential of a parameterization and check whether it is conformal. In particular, we prove that the stereographic projection is conformal.

2.3   The Normal Vector or Gauß Map

Consider a surface parameterization $\phi : \Omega \to \mathbb{R}^3$. For each point $p \in \Omega$ and two coordinate vectors $U = \frac{\partial}{\partial u}, V = \frac{\partial}{\partial v}$, the vectors $d\phi(p) \cdot U, d\phi(p) \cdot V$ span a linear subspace of $\mathbb{R}^2$, the tangent space of Σ at $\phi(p)$.

Orthogonal to this tangent space is a unit vector in $\mathbb{R}^3$ which is used to define an important map from Ω into the unit sphere:

Definition **2.5** *The normal vector to the tangent space is called the Gauß map:*

$$
\begin{aligned}
N : \Omega &\rightarrow S^2 \\
N(p) &= \left. \frac{d\phi \cdot U \times d\phi \cdot V}{|d\phi \cdot U| \cdot |d\phi \cdot V|} \right|_p
\end{aligned}
$$

Remark **2.2** There is an ambiguity here as there are two different normal vectors which point in opposite directions. This can be helped by fixing once

9

and for all orientations of the domain $\Omega \subset \mathbb{R}^2$ and $\mathbb{R}^3$. Then the normal vector is chosen so that for an oriented basis U, V of the tangent space to some point p of Ω at some point, the vectors $d\phi U, d\phi V, n$ form an oriented basis of the tangent $\mathbb{R}^3$ at $\phi(p)$.

So far we have only considered first order derivatives of the surface parameterization (to write down tangent vectors). The second order derivatives lead to important geometric data, called curvatures. Here is what we need:

Definition 2.6 *The Weingarten map or shape operator S is defined as*

$$d\phi \cdot S \cdot V = dN \cdot V$$

In this definition, we have identified the tangent space of the surface at $\phi(p)$ with the tangent space of the unit sphere at $n(p)$ by a parallel translation.

Proposition 2.1 *The Weingarten map is a symmetric endomorphism of the tangent spaces of Ω with respect to the Riemannian metric g.*

Definition 2.7 *The eigenvalues of the Weingarten map are called principle curvatures. The eigendirections indicate where the surface bends most and least. The principle curvatures are combined into mean curvature*
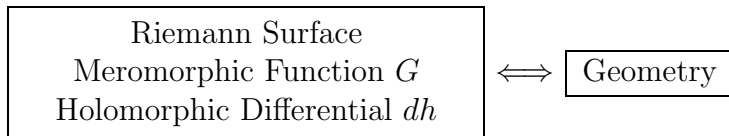
$$H = \operatorname{trace} S$$

and Gauß curvature

$$K = \det S$$

3 The Weierstrass Representation

Our goal will be to understand the following interaction:

| Riemann Surface
Meromorphic Function G
Holomorphic Differential dh | $\Longleftrightarrow$ | Geometry |

3.1 The Gauß map

A minimal surface in $\mathbb{R}^3$ is a surface which locally minimizes area. In this sense it is a two-dimensional generalization of a straight line, a path which locally minimizes arc length. To make this precise and achieve minimal completeness of exposition, we give the definition of area even though we won't need it later on:

Definition 3.1 *The area of a surface Σ, parametrized by $\phi : \Omega \to \mathbb{R}^3$, is defined as*

$$\text{area}(\Sigma) = \int_\Omega dA$$

Here dA is the area form (or density) of the surface. Using coordinates (x_1, x_2) of Ω and coordinate tangent vectors $X_j = \frac{\partial}{\partial x_j}$

$$dA = (\det g(d\phi X_i, d\phi X_j))^{\frac{1}{2}} \, dx_1 dx_2$$

Equivalently, for minimal surfaces, the Gauss map is anticonformal. This means: It preserves angles and changes the orientation.

Proof: The mean curvature being zero implies that S has eigenvalues $\lambda \geq 0$ and $-\lambda$. Thus the square of S is equal to $\lambda^2 id$. Hence

$$
\begin{aligned}
\langle dnU, dnU \rangle &= \langle d\phi SU, d\phi SU \rangle \\
&= g(SU, SU) \\
&= g(S^2 U, U) \\
&= \lambda^2 g(U, U)
\end{aligned}
$$

This implies that the Gauß map preserves angles. It reverses the orientation, because for a positively oriented basis of curvature directions,

$$\det(dnU, dnV, n) = \det(d\phi SU, d\phi SV, n)$$

$$
\begin{aligned}
&= \det(\lambda d\phi U, -\lambda d\phi V, n) \\
&= -\lambda^2 \det(d\phi U, d\phi V, n) \\
&\leq 0
\end{aligned}
$$

because, by definition, $d\phi U, d\phi V, n$ are positively oriented in $\mathbb{R}^3$. $\qquad\qquad \square$

Precomposing the Gauss map with a conformal parameterization of the surface and postcomposing it with an anticonformal stereographic projection, yields a conformal map from the domain of definition of the surface to the Riemann sphere. This meromorphic function is denoted by G and called the Gauss map as well.
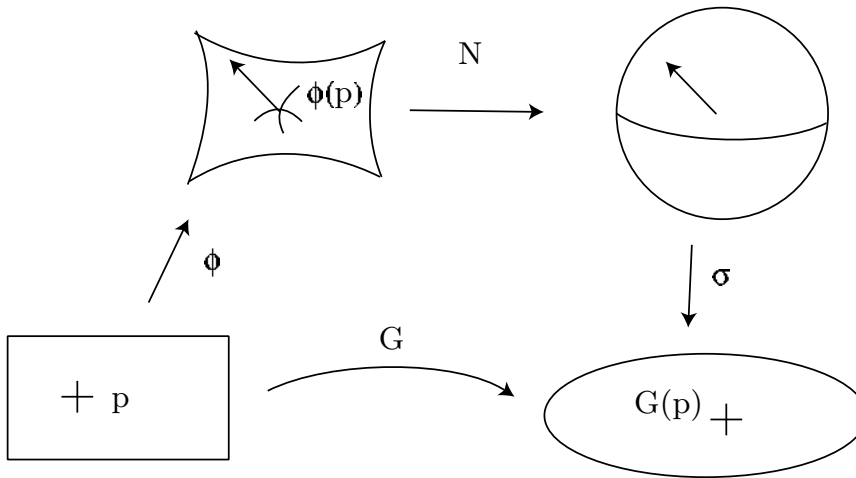
Figure 2: The Gauss map

3.2   Harmonic coordinate functions

Consider a conformally parametrized surface

$$
\begin{aligned}
\phi : U &\rightarrow \mathbb{R}^3 \\
z = u + iv &\mapsto (x_1, x_2, x_3)
\end{aligned}
$$

This surface is minimal if and only if the coordinate functions are harmonic, that is if they satisfy

$$
\Delta x_i = \left(\frac{\partial^2}{\partial u^2} + \frac{\partial^2}{\partial v^2} \right) x_i = 0
$$

In the domain U of definition, the harmonic coordinate differentials dx_i possess holomorphic extensions. It is customary to denote the holomorphic

extension of the third coordinate differential dx_3 by dh and to call it the height differential. We have

$$dx_3 = \operatorname{Re} dh$$

3.3   Weierstrass data

Now suppose that we are given a conformal minimal surface parameterization $\phi = (\phi_1, \phi_2, \phi_3)$, defined in a domain Ω. As the ϕ_j are harmonic functions in Ω, we can write them locally as the real parts of holomorphic functions. Or, globally, as

$$\phi = \operatorname{Re} \int^p (\omega_1, \omega_2, \omega_3)$$

with holomorphic 1-forms ω_j defined in all of Ω. Suppose, on the other hand, we are given such a parameterization. This is conformal (and hence parameterizes a minimal surface) if and only if

$$\omega_1^2 + \omega_2^2 + \omega_3^2 \equiv 0$$

in Ω. The conformal factor λ^2 is given by

$$\lambda^2 = |\omega_1|^2 + |\omega_2|^2 + |\omega_3|^2 \tag{2}$$

Together we have

Theorem 3.1 *Given holomorphic forms $\omega_1, \omega_2, \omega_3$ in Ω such that*

$$\omega_1^2 + \omega_2^2 + \omega_3^2 \equiv 0$$

and

$$|\omega_1|^2 + |\omega_2|^2 + |\omega_3|^2 \neq 0$$

Then

$$\phi(p) = \operatorname{Re} \int^p (\omega_1, \omega_2, \omega_3)$$

defines a conformally parametrized minimal surface in $\mathbb{R}^3$, and every conformal minimal surface parameterization arises this way.

We call the $\int \omega_j$ the holomorphic extensions of the coordinate functions.

We have associated two pieces of holomorphic data to a conformally parametrized minimal surface so far, namely its Gauß map and the holomorphic extensions of the coordinate functions. Because the Gauß map can be expressed in terms of the tangent vectors, it is natural to expect that the meromorphic function G can be written in terms of the holomorphic coordinate differentials.

In fact, using the formula for the stereographic projection (1), one obtains

$$G = \frac{-\omega_1 + i\omega_2}{\omega_3}$$

This allows us to use meromorphic data G and $dh = \omega_3$ defined in a domain Ω to write down the surface parameterization in the so-called Weierstraß representation

$$\phi(z) = \text{Re} \int^z \left(\frac{1}{2} \left(\frac{1}{G} - G \right), \frac{i}{2} \left(\frac{1}{G} + G \right), 1 \right) dh \qquad (3)$$

Observe that this integral might (and frequently will) depend on the path of integration if the domain Ω is not simply connected.

As explained, G depends on the choice of the stereographic projection, and dh depends how we rotate the surface in space. However, a different choice changes G and dh only by a fractional linear transformation.

We will treat G and dh as the two basic holomorphic objects associated to a minimal surface. One of our main goals will be to understand how the geometry of a minimal surface is related to complex-analytic properties of G and dh.

14

3.4   The first examples
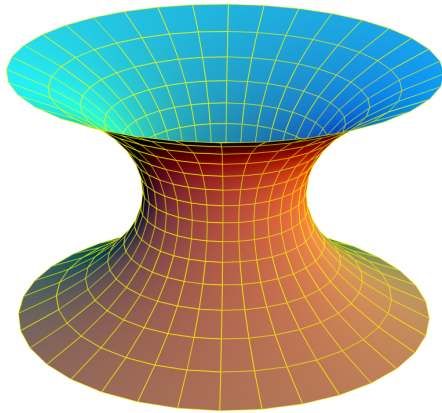
Figure 3: The Catenoid

Example **3.1 (The Catenoid and Helicoid)** The catenoid is the only minimal surface of revolution:

$$G(z) = z \tag{4}$$
$$dh = \frac{1}{z}dz \tag{5}$$

Integrating these data gives the parameterization

$$\phi(z) = \mathrm{Re}\left(-\frac{1}{2}(\frac{1}{G} + G), \frac{i}{2}(G - \frac{1}{G}), \log z\right)$$

in $\Omega = \mathbb{C}^*$. Observe that while $\log z$ is not well-defined in Ω, its real part is.

and the Helicoid is the only ruled minimal surface:

$$G(z) = z \tag{6}$$
$$dh = \frac{i}{z}dz \tag{7}$$

Figure 4: The Helicoid

Integrating these data according to (3) gives the parameterization

$$\phi(z) = \mathrm{Re}\left(-\frac{i}{2}(\frac{1}{G} + G), -\frac{1}{2}(G - \frac{1}{G}), i\log z\right)$$

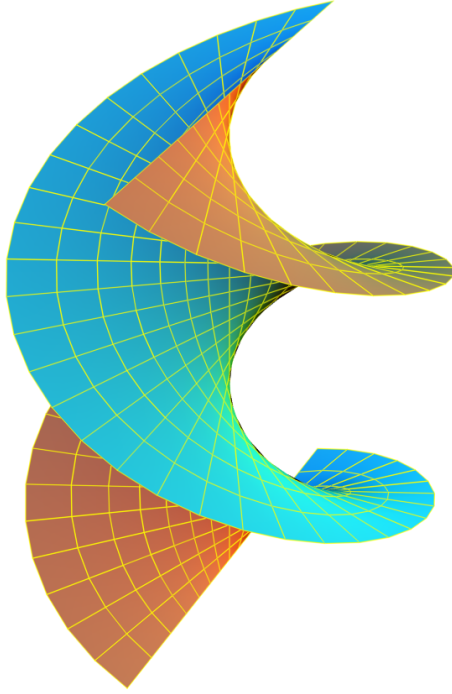Here we face for the first time a problem which will become more and more prominent: While the data G and dh are well-defined in all of $\Omega = \mathbb{C}^*$, the integral $\mathrm{Re}\int^z \omega_3$ depends on the homotopy class of the path of integration. The effect is visible in the figure: The images of the same point in Ω reached by different paths differ by a vertical translation which is a multiple of 2π.

Technically, there are three ways out of this problem: We can restrict the domain Ω to a simply connected subset of Ω, we can use the universal cover of Ω, or we can consider surfaces into space forms $\mathbb{R}^3/\Gamma$.

Example 3.2 (The Enneper surface) Taking

$$G(z) = z, dh = zdz \tag{8}$$

in the euclidean plane defines the Enneper surface. Integrating the formula (3) gives the surface parameterization

$$\phi(z) = \mathrm{Re}\left(\frac{1}{2}\left(z - \frac{z^3}{3}\right), \frac{i}{2}\left(z + \frac{z^3}{3}\right), \frac{z^2}{2}\right)$$

16

The surface has two horizontal straight lines on which are the horizontal diagonals $y = \pm x, z = 0$. You can rotate the surface about them into itself. There are also reflectional symmetries about the two vertical coordinate planes.

Below are two pictures. The first shows a portion near the origin which is still without self-intersections, the second features the end. One can see clearly that the Gauß map has degree 3 at infinity.
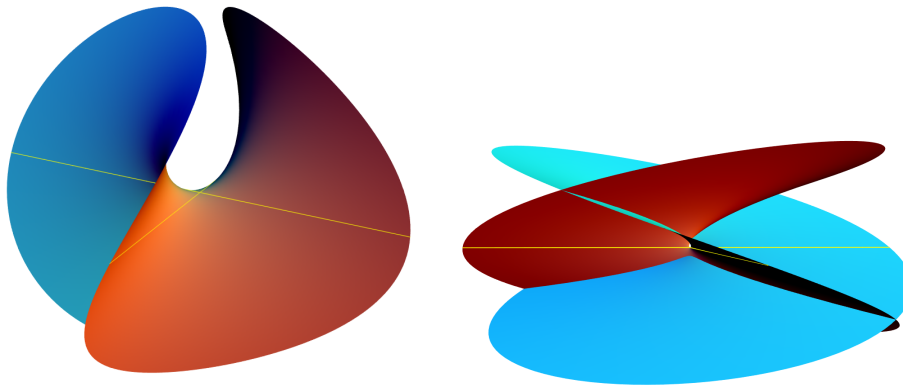
Figure 5: Different portions of the Enneper surface

Mathematica Notebook **3.3** The Mathematica notebook *Weierstrass.nb* shows how to integrate simple Weierstraß data and to plot the minimal surfaces.

3.5   Local analysis at regular points

We begin our discussion of the relationship between holomorphic properties of the Weierstraß data and geometric properties of the minimal surface at regular points of the surface.

Suppose that a minimal surface is given by a conformal parameterization ϕ in a domain Ω. We have seen that this parameterization ϕ can be written in terms of data G and dh where the height differential dh is a holomorphic 1-form in Ω, and the Gauß map is a meromorphic function.

The Riemanninan metric of a minimal surface can be computed in terms of the Weierstraß data by (2) and (3)

$$ds = \frac{1}{2}\left(|G| + \frac{1}{|G|}\right)|dh| \qquad (9)$$

This is precisely the conformal stretch factor of the isothermal surface parameterization. For a point $p \in \Omega$ to parameterize a regular surface point, this factor must be finite and non-zero. Hence there is a balancing condition for the orders of G and dg at regular points, namely

Proposition 3.1 *At a regular point, G has a zero or pole of order n at p if and only if dh has a zero of order n.*

Otherwise, the metric would either become singular (zero or infinite) at p.

Exercise 3.2 *Devise simple examples of this situation and plot the corresponding surface. You can use he notebook weierstrass.nb as a starting point.*

Example 3.4 (Surfaces defined on the entire complex plane) Let $P(z)$ and $Q(z)$ be two entire functions. Then

$$\begin{aligned} G(z) &= \frac{P(z)}{Q(z)} \\ dh &= P(z) \cdot Q(z) \end{aligned}$$

provides Weierstraß data of a minimal surface so that all complex numbers are regular points. A very special case is given by $P(z) = z^k$ and $Q(z) = 1$. These surfaces are Enneper surfaces of higher dihedral symmetry. (Recall that the dihedral symmetry group is the symmetry group of a regular n-gon. Many minimal surfaces contain such a symmetry group).
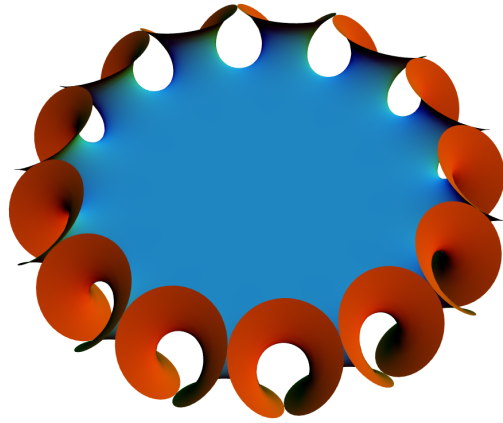
Figure 6: Enneper surface of order 12

Exercise 3.3 *Represent the catenoid and the helicoid in this way. Hint: Use $G(z) = e^z$. Why is this possible, even though the catenoid appears to have two ends?*

Mathematica Notebook 3.5 The Notebook *OneEnd.nb* discusses further examples of this type.

3.6   The associate family

For any minimal surface Σ given by G and dh, there is a natural 1-parameter deformation Σ^t of minimal surfaces associated to it, given by G and $e^{it}dh$. The parameterization is given locally by

$$\phi^t : z \mapsto \mathrm{Re} \int^z e^{it}(\omega_1, \omega_2, \omega_3)$$

This family Σ^t of minimal surfaces is called the associate family of Σ.

All surfaces Σ^t are isometric minimal surfaces, as the square of the conformal factor of the Riemannian metric is given by

$$ds^2 = |\omega_1|^2 + |\omega_2|^2 + |\omega_2|^2$$

and thus independent of t. This has the consequence that the deformation can be carried out physically without tearing or stretching.

Also, the Σ^t have the same Gauß map by definition.

3.7   The conjugate surface and symmetries

Of particular importance is the conjugate surface

$$\Sigma^* = \Sigma^{\pi/2}.$$

The simplest example of such a conjugate pair is the catenoid and the helicoid. The second simplest pair is the singly and doubly periodic Scherk surface.

Many important examples of minimal surfaces have extrinsic symmetries, that is, they are invariant under rotations about straight lines and reflections at planes. The curves which are fixed under these symmetries are landmarks of a minimal surface.

Exercise 3.4 *The associate family of the Enneper surface is a 1-parameter family of isometric surfaces in space. Show that the Enneper surface and its conjugate are isometric through a euclidean motion. This is not the case for two general members of the associate family.* $\mathbb{R}^3$.

Definition 3.2 *Let Σ be a surface. A planar symmetry line is curve on Σ which lies in a plane orthogonal to the surface everywhere along the curve. A straight symmetry line is a straight line lying entirely on Σ.*

Exercise 3.5 *Discuss the symmetry lines of the catenoid and the helicoid.*

Using the Schwarz reflection principle for harmonic functions, a minimal surface which is bounded by a symmetry line of either kind can be continued by reflecting or rotating it about this line. The resulting surface will automatically be a smooth minimal surface.

This is very important, because many minimal surfaces can be decomposed by their symmetries into simply connected pieces which are simpler to deal with. Moreover, for drawing minimal surfaces, it requires less work to compute only the image of such a a fundamental piece.

Furthermore, there is an intimate relationship between the two types of symmetry lines on a minimal surface and on its conjugate:

Proposition 3.6 *A planar symmetry line for Σ becomes a straight symmetry line for Σ^* and vice versa. Under this correspondence, the normal vector of the symmetry plane becomes the direction vector of the straight line.*

The conjugate minimal surface plays also an important role in the construction of minimal surfaces or in proving their embeddednes. For more details, see [Kar89].

4 Minimal surfaces on Punctured Spheres

We will discuss elementary properties of minimal surfaces and discuss a few examples defined on punctured spheres. It is a consequence of the López-Ros theorem (see [LR91]) that there are no complete embedded minimal surface parameterized by punctured spheres besides the plane and the catenoid. Nevertheless, these surfaces can teach us a great deal about the construction of minimal surfaces, because one of the principle difficulties, the closing of the periods, is relevant but easy to overcome.

4.1 Period conditions

For a minimal surface given by holomorphic Weierstrass data $\omega = (\omega_1, \omega_2, \omega_3)$ on a domain X, the actual parameterization is obtained by the map

$$z \mapsto \operatorname{Re} \int^z \omega$$

For this to be a single valued map on the domain, we need that closed curve in the domain are being mapped to closed curve on the surface. This is automatically true only for curves which are homologous to 0. In general, we want the following period condition to hold:

$$\operatorname{Re} \int_\gamma \omega = 0 \qquad \forall \gamma \in H_1(X, \mathbb{Z})$$

In many important cases the geometry of the minimal surface has preferred directions in euclidean space. For instance, if there are parallel ends, their common normal vector is such a preferred direction. Or, if there is translational period, this is also a preferred direction. The Weierstrass representation often becomes simpler when such preferred directions are used as the coordinate vectors.

It is frequently helpful to look at the Weierstrass representation forms Gdh and $\frac{1}{G}dh$ instead of at the forms ω_1 and ω_2. The period conditions can then be stated as

$$\int_\gamma Gdh = \overline{\int_\gamma \frac{1}{G}dh} \tag{10}$$

$$\operatorname{Re} \int_\gamma dh = 0 \tag{11}$$

for all cycles γ on X.

We will call the first condition the horizontal period condition and the second the vertical period condition.

4.2   A surface with a planar end and an Enneper end

We begin our list of examples with a minimal surfaces which i sparameterized by a punctured plane, with one puncture at 0 corresponding to a planar end and the puncture at ∞ corresponding to an Enneper end. This surface has no further ends. To achieve this, we make sure that the conformal stretch factors at the ends have the correct asymptottic behavior. For the Enneper end, recall the Weierstraß representation of the Enneper surface with an end of order k was given in example (3.4)

$$G(z) = z^k, dh = z^k dz$$

so that the conformal stretch factor near infinity becomes

$$ds \sim |z^{2k}| \cdot |dz|$$

Hence if we choose

$$
\begin{aligned}
G(z) &= z^3 \\
dh &= z dz
\end{aligned}
$$

this surface will have an Enneper end of order 2 at infinity, and the puncture at 0 represents a planar end. To see this, we write $z = 1/w$ and obtain $G(w) = w^3, dh = -w^{-3} dw$ so that near $w = \infty$ we get $ds \sim |dw|$ so that the metric becomes euclidean. Note that a planar end is distinguished from a catenoidal end (which has also euclidean growth) by the vanishing of the logarithmic growth rate, which is the residue of dh.
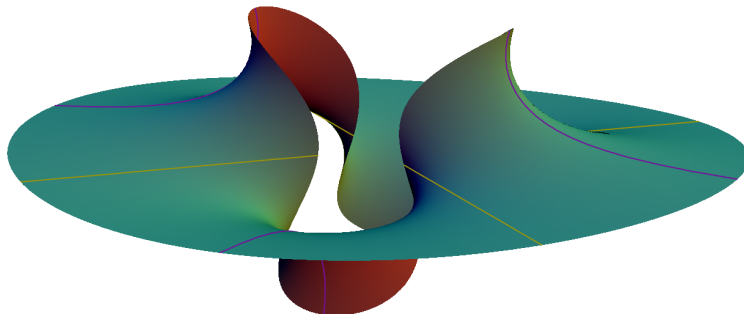

Figure 7: A sphere with two ends

4.3 A sphere with one planar and two catenoid ends

This example shows how the attempt to find a minimal sphere with three parallel embedded ends fails.
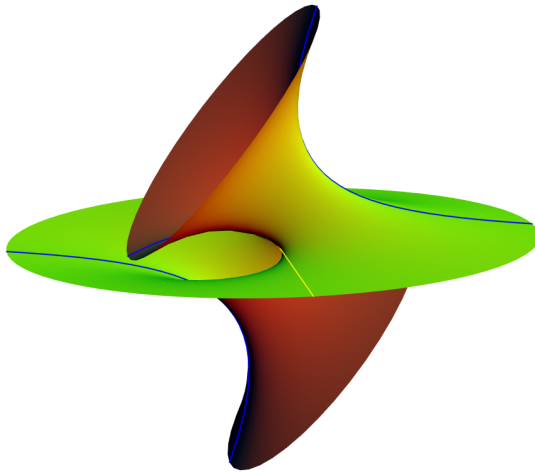

Figure 8: A sphere with three ends

We are looking for a sphere with three ends, one of them planar, the other two catenoidal. Let's arrange the surface so that the Gauß map at the two catenoid ends is vertical and has two simple poles. The same will then hold for the height differential, with the residues being real.

We won't assume anything about the Gauß map at the planar end, so that we can find out whether it might be vertical.

Next let's normalize the parameter sphere so that the planar end is represented by infinity and the two catenoid ends by ± 1.

As we want a straight line on the surface, this line corresponds to the imaginary axes, and the Gauß map must be real on it.

So far we have shown that the Weierstraß representation is of the form

$$
\begin{aligned}
G(z) &= \rho \frac{az^2 + bz + c}{z^2 - 1} \\
dh &= \frac{az^2 + bz + c}{z^2 - 1} dz
\end{aligned}
$$

The condition that the Gauß map is real on the imaginary axes forces $b = 0$.

The vertical period condition at ∞ becomes

$$\operatorname*{res}_{z=\infty} dh = -b = 0$$

so that we have $b = 0$. As the form $\frac{1}{G}dh = \frac{1}{\rho}dz$ is exact, the vertical and horizontal period conditions for cycles around ± 1 become

$$\operatorname*{res}_{z=\pm 1} Gdh = \pm\frac{1}{4}(3a - c)(a + c)\rho = 0$$
$$\operatorname*{res}_{z=\pm 1} dh = \pm\frac{1}{2}(a + c) = 0$$

Hence $c = 3a$. Furthermore, a can't vanish, because then also $c = 0$, and the Weierstraß data would degenerate. Without loss we can assume that $a = 1$ and $c = 3$. This solves all period conditions and leaves us with a free parameter, the positive López-Ros parameter ρ. This is also the value of the Gauß map at ∞, the planar end. As this parameter can't be 0 without that the Weierstraß data degenerate, the Gauß map can't be vertical at the planar end. Hence the ends will never be parallel and must intersect eventually. Observe that the Weierstraß data are exact in this case.
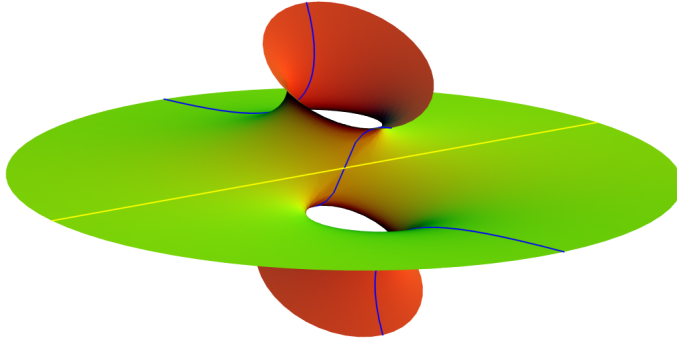

Figure 9: Another sphere with three ends

4.4 The k-Noids of Jorge and Meeks

Let us try to find the Weierstraß data of a minimal surface Σ_k which looks like the surface below for $k = 6$:
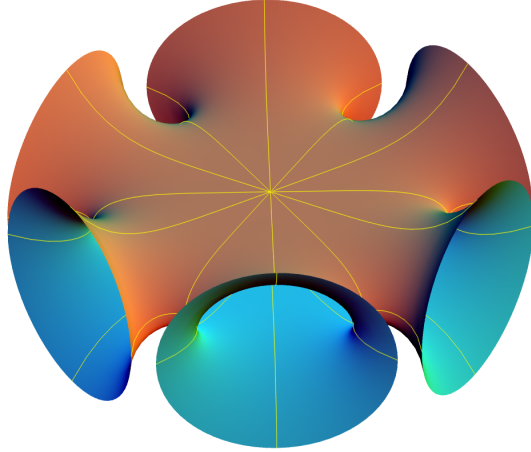
Figure 10: A Jorge-Meeks 6-Noid

Topologically, this is a sphere with k holes. As each of the ends should be a catenoid end, we expect the underlying domain to be a sphere, punctured at k points p_k representing the ends. Assuming a rotational symmetry, we can choose these points to be the kth roots of unity. We see and hope that the Gauss map is only vertical at the intersection of the surface with the z-axes. Again by symmetry, these two points correspond to 0 and ∞. Thus we expect $G(z) = \rho z^m$ for some integer m. Near a point where the Gauss map has degree m, the surface looks like an umbrella with $m+1$ valleys and $m+1$ ridges. Hence we obtain

$$G(z) = \rho z^{k-1}$$

with ρ to be determined. Now let's turn to the height differential. We claim that it has to be

$$dh = \lambda \frac{z^{k-1}}{(z^k - 1)^2} dz$$

This is because we need dh to have zeroes of order $k-1$ at 0 and ∞ to make these points regular and we need single order poles at the p_k to make these points represent catenoidal ends. From the residues

$$\begin{aligned}
\operatorname*{res}_{z=1} G dh &= \lambda \frac{(k-1)\,\rho}{k^2} \\
\operatorname*{res}_{z=1} \frac{1}{G} dh &= \lambda \frac{1-k}{k^2\,\rho} \\
\operatorname*{res}_{z=1} dh &= 0
\end{aligned}$$

and the period condition we conclude that

$$|\rho|^2 = \overline{\lambda}/\lambda$$

so that we can and have to choose without loss $\lambda = 1$ and $\rho = 1$.

26

Exercise 4.1 *Verify that for $k = 2$ we get a surface which is isometric to the catenoid.*

5 The Scherk Surfaces

We discuss the classical Scherk surfaces and some of its variations

5.1 The singly periodic Scherk surface

The singly periodic Scherk surface is defined on the four-punctured sphere $\widehat{\mathbb{C}} - \{\pm 1, \pm i\}$ by the meromorphic Weierstrass data

$$
\begin{aligned}
G(w) &= w \\
dh &= \frac{i\,w}{w^4 - 1}dw
\end{aligned}
$$
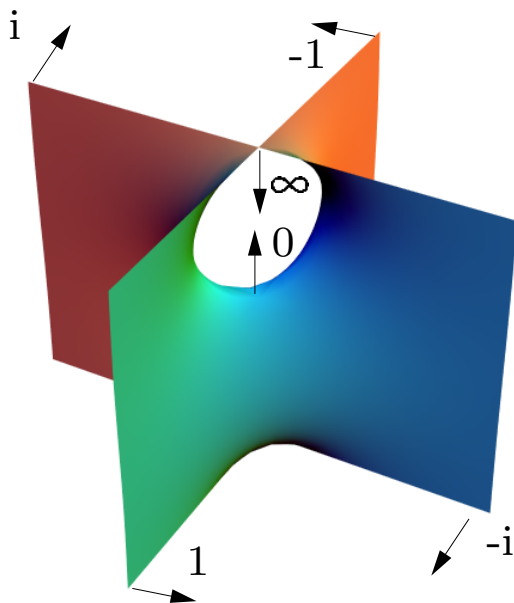
Figure 11: A fundamental piece of Scherk's singly periodic surface

As the Gauss map is the identity map, surface points with known normal vectors can easily be spotted in the parameter sphere.

5.2 The period conditions

For the singly periodic Scherk surface, closed curves γ in $\widehat{\mathbb{C}} - \{\pm 1, \pm i\}$ are mapped by the parameterization to curves connecting points on the surface which are equivalent under vertical translations.

On the other hand, the Weierstrass representation tells us that the difference vector of two such points is given by the real part of the so-called period vector

$$\oint_\gamma \left(\frac{1}{2}\left(\frac{1}{G} - G \right) dh, \frac{i}{2}\left(\frac{1}{G} + G \right), dh \right)$$

As any curve on the surface is homologous to cycles around the punctures, it suffices to check that this period vector is an integral multiple of a fixed vertical vector for closed curves around the punctures $\epsilon \in \{\pm 1, \pm i\}$. These integrals can be evaluated by the residue theorem:

1. Vertical periods:

$$\oint_\epsilon dh = 2\pi i \operatorname*{res}_{w=\epsilon} \frac{iw}{w^4 - 1} dw = -\frac{\pi}{2\epsilon^2} \in \left\{ \pm \frac{\pi}{2} \right\}$$

2. Horizontal periods:

$$
\begin{aligned}
\oint_\epsilon G dh &= 2\pi i \operatorname*{res}_{w=\epsilon} \frac{iw^2}{w^4 - 1} dw = -\frac{\pi}{2\epsilon} \\
\oint_\epsilon \frac{1}{G} dh &= 2\pi i \operatorname*{res}_{w=\epsilon} \frac{i}{w^4 - 1} dw = -\frac{\pi}{2\epsilon^3}
\end{aligned}
$$

As $\epsilon \in \{\pm 1, \pm i\}$, we have indeed

$$\operatorname{Re} \oint_\epsilon \left(\frac{1}{G} - G \right) dh = 0 = \operatorname{Re} \oint_\epsilon i \left(\frac{1}{G} + G \right) dh$$

This last horizontal condition can be stated equivalently as

$$\oint_\epsilon G dh = \overline{\oint_\epsilon \frac{1}{G} dh}$$

Scherk's formula of this surface as a graph is

$$\cos z = \cos^2(\phi) \cdot \cosh \frac{x}{\cos\phi} - \sin^2(\phi) \cdot \cosh \frac{y}{\cos\phi}$$

Here ϕ is a free paramater which measures half of the angle between the planar ends. In our case we have $\phi = \frac{\pi}{2}$.

As explained, the coordinate functions of a minimal surface are harmonic and hence possess locally holomorphic extensions. It turns out that

the mapping behavior of the complex coordinate maps

$$z \mapsto \int^z G dh$$

$$z \mapsto \int^z \frac{1}{G} dh$$

is very often surprisingly simple.

For the singly periodic Scherk surface, the restrictions of these maps to the first quadrant have the following image domains, consisting each of two orthogonal half-infinite parallel strips of the same width:
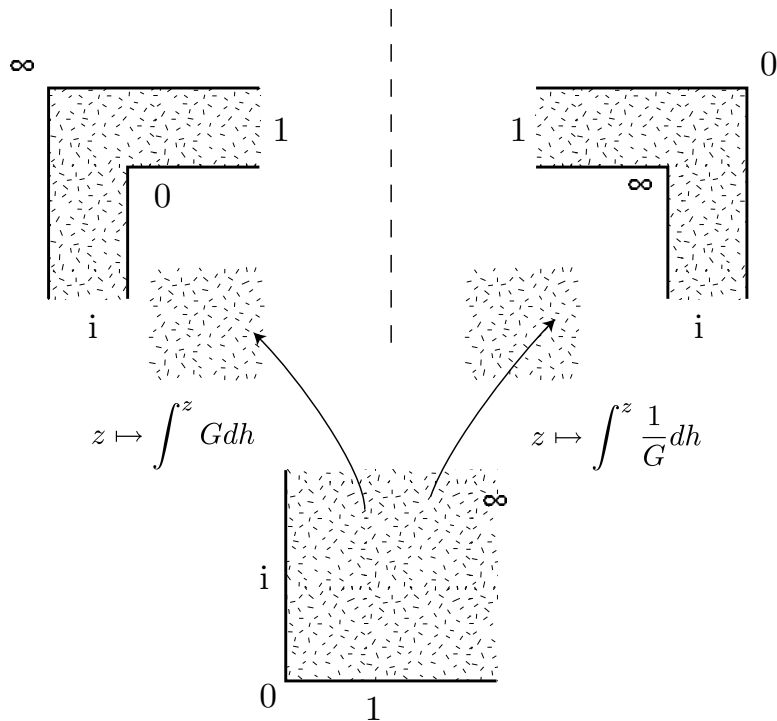
Figure 12: Image of the first quadrant under complex coordinate maps

This follows from the Schwarz-Christoffel formula (see section 5.7). It is a rather surprising phenomenon that the relatively complicated minimal surface patch can be understood through pieces which have an elementary geometric description. We will explain and exploit this later again.

5.3 Changing the angle between the ends

As was already observed by Scherk, the angle between the ends can be varied both for the singly and the doubly periodic surface. Here is the

Weierstraß representation for the singly periodic surface:

$$
\begin{aligned}
G(z) &= z \\
dh &= \frac{dz}{z(z^2 + 1/z^2 - 2\cos 2\phi)} \\
&= \frac{dz}{(z^2 - e^{i2\phi})(z^2 - e^{-i2\phi})}
\end{aligned}
$$

The angle ϕ is half the angle between the Scherk ends, it varies between 0 and $\frac{\pi}{2}$. For $\phi = \frac{\pi}{4}$, we get the classical Scherk surfaces with orthogonal ends.

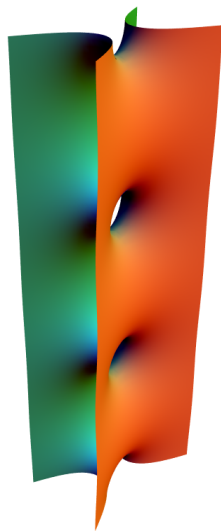**Exercise 5.1** *What do the period conditions mean in terms of figure 13?*

Figure 13: A sheared singly periodic Scherk surface

Exercise 5.2 *Verify that the period conditions are satisfied.*

Exercise 5.3 *What happens for $\phi \to 0$?*

5.4   The doubly periodic Scherk surface

Scherk wrote down his doubly periodic surface as a graph over the square $Q = (-\frac{\pi}{2}, \frac{\pi}{2}) \times (-\frac{\pi}{2}, \frac{\pi}{2})$:

$$e^z = \frac{\cos y}{\cos x}$$

The same formula defines a translation-invariant graph over all squares $Q + \pi k + \pi i l$ with $k + l \equiv 0 \pmod 2$ (think of these squares as the black squares of a checkerboard tessellation of the plane).

This parameterization is not very well suited for creating images of the surface. It is not conformal, and it doesn't behave nicely at the ends. Also, it doesn't show that the translational copies of the graph fit together along vertical straight lines over the corners of the squares.
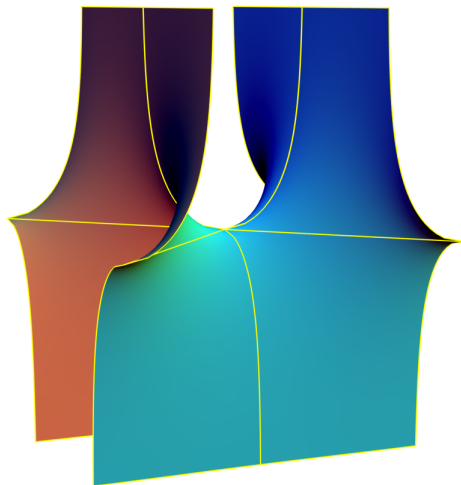
Figure 14: A fundamental piece of Scherk's doubly periodic surface

How can we find a (better) conformal parameterization of the surface?

Mathematica Notebook 5.1 In the notebook *Scherk.nb*, we take the above surface parameterization and compute the Gauß map. The inverse of this map composed with the surface parameterization gives a conformal surface parameterization. This is used to derive a Weierstraß representation of the surface.

Here we will follow a more geometrical approach: Let's look at a fundamental piece of the surface, divided by its translational symmetries. It

is cut into eight congruent curved pieces by straight and planar symmetry lines. In the parameterization of the surface patch as a graph over the square $(-\frac{\pi}{2}, \frac{\pi}{2}) \times (-\frac{\pi}{2}, \frac{\pi}{2})$, these lines correspond to the diagonals and medians of the square. Note that the horizontal curves are not symmetry curves, these arise from cutting off the ends of the surface. Each of these three boundary curves is mapped by the normal map to a quarter of a great circle in the image S^2, and the curves intersect under $\pi/4$ angles. Hence the symmetry curves are mapped by the Gauss map to the octahedron tessellation of the round sphere. The round S^2 is identified with the Riemann sphere so that the four ends of the surface become the fourth roots of unity (we might need to rotate the surface for this to hold), and the center point of the piece is mapped to 0, while the four (identified) corners are mapped to ∞.

If we use this Riemann sphere as a new domain to parameterize the surface, the Gauss map will just be the identity map.

The height differential will be a meromorphic 1-form on this Riemann sphere with two simple zeroes at 0 and ∞ where the Gauss map is vertical. As the sum of the orders of the zeroes and poles of a meromorphic form on the Riemann sphere is -2, we need to distribute 4 simple poles. We are forced to put these at the ends. Hence

$$
\begin{aligned}
G(z) &= z \\
dh &= \lambda \frac{z}{z^4 - 1} dz
\end{aligned}
$$

It remains to determine λ. As

$$
\operatorname*{res}_{z=1} dz = \frac{\lambda}{4}
$$

the ends cause no vertical periods if and only if λ is real. Without loss, we can put $\lambda = 1$. Observe that

$$
\operatorname*{res}_{z=1} G dz = \operatorname*{res}_{z=1} \frac{1}{G} dz = \frac{1}{4}
$$

so that each end produces horizontal periods, as wanted. So we see that Scherk's doubly periodic minimal surface is conjugate to his singly periodic surface. Scherk didn't know this, because the notion of conjugate surfaces was only discovered later.

By looking at the conjugate of Scherk's singly periodic surface with arbitrary angle between the ends, one obtains sheared Scherk surfaces like the one in figure 15. Lazard-Holy and Meeks ([LHI98]) have shown that these are the only doubly periodic surfaces of genus 0.
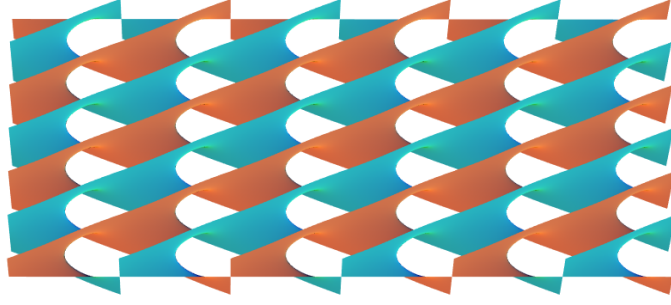
Figure 15: A sheared doubly periodic Scherk surface

5.5 Singly periodic Scherk surfaces with higher dihedral symmetry

We will now produce singly periodic Scherk surfaces with higher dihedral symmetry in the same way as we got the Enneper surfaces of higher symmetry. Here is the Weierstraß representation for $2k$-ended surfaces, with an additional parameter ϕ:

$$
\begin{aligned}
G(z) &= z^{k-1} \\
dh &= \frac{dz}{z(z^k + 1/z^k - 2\cos k\phi)} \\
&= \frac{z^{k-1}dz}{(z^k - e^{ik\phi})(z^k - e^{-ik\phi})}
\end{aligned}
$$

These surfaces are embedded as long as

$$
\frac{\pi}{2} - \frac{\pi}{k} < (k-1)\phi < \frac{\pi}{2}
$$

This condition ensures that the planar ends do not intersect. The most symmetric case, where the asymptotic planes of neighboring ends intersect at the same angle $\frac{\pi}{k}$, is obtained for $\phi = \frac{\pi}{2k}$.

34
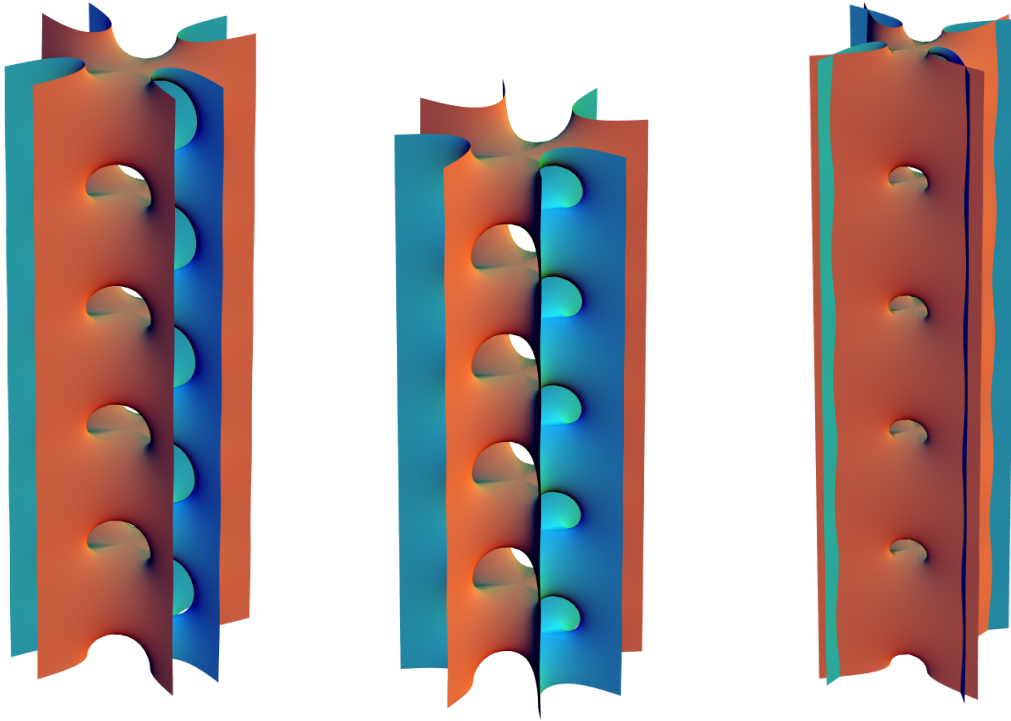
Figure 16: Singly periodic Scherk surface with eight ends

Exercise 5.4 *Verify the last claim.*

Observe that for $\phi = 0$, we obtain the Weierstrass representation of the Jorge-Meeks surfaces. One can see this convergence geometrically if one rescales the surfaces correctly. The right figure of 16 show a Scherk surface close to several very large 4-noids.

One can even obtain less symmetric Scherk-like surfaces, using a conjugate Plateau construction in combination with a theorem of Jenkins and Serrin, see [Kar88, JS66].

5.6 The twist deformation of Scherk's singly periodic surface

There is another, more complicated deformation of the singly periodic Scherk surfaces ([Kar88]):

Figure 17: Singly periodic Scherk surface with four helicoidal ends

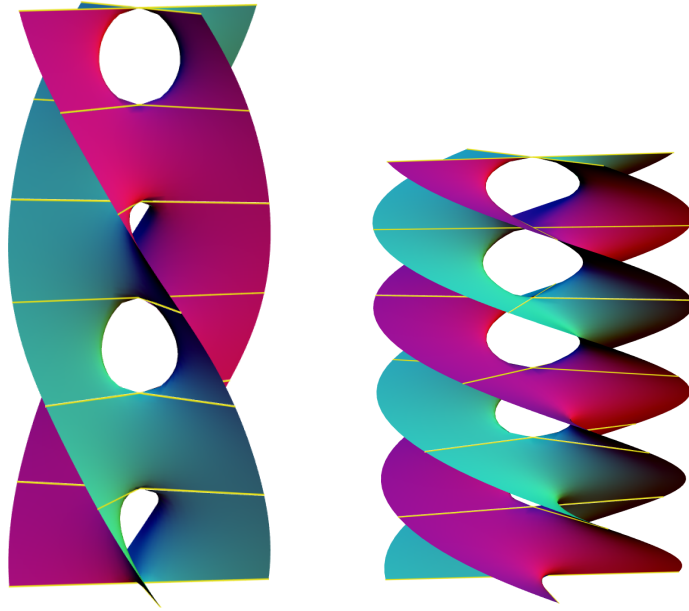These twisted Karcher-Scherk surfaces can be obtained from the classical Scherk surface by twisting them about the vertical coordinate axes. They are invariant under a vertical screw motion with twist angle $\alpha = a\pi$ and exist for $0 \leq a < \frac{1}{2}$. The quotient surface is again a four-punctured sphere with punctures at $\pm R, \pm i/R$, where R is a real parameter to be determined so that a horizontal period condition is satisfied. While the height differential is still quite simple, the Gauss map is more complicated. Here is the formula from [Kar88]:

$$
\begin{aligned}
G(w) &= w \cdot \left(\frac{w^2 - R^2}{R^2 w^2 + 1} \right)^a \\
dh &= \frac{iw}{(w^2 - R^2)(R^2 w^2 + 1)} dw
\end{aligned}
$$

For $a = 0$ and $R = 1$, we obtain the classical Scherk surface.

The Gauß map has the feature that it is not anymore single valued on the quotient surface, and this makes a discussion of the horizontal period problem for this surface a bit painful.

Instead of doing this, we will use a different approach which uses Schwarz-Christoffel maps. This map allows to write down maps from the upper half plane to euclidean polygons and has become an important tool in constructing Weierstraß data. The following section 5.7 will discuss this formula briefly.

We begin with an elementary construction:

For $0 < a < \frac{1}{2}$, construct a right-angled triangle with angles $(\frac{1}{4} - \frac{a}{2})\pi$ and $(\frac{1}{4} + \frac{a}{2})\pi$. Reflect it at the hypothenuse and extend the edges to infinity. Color the edges as indicated:
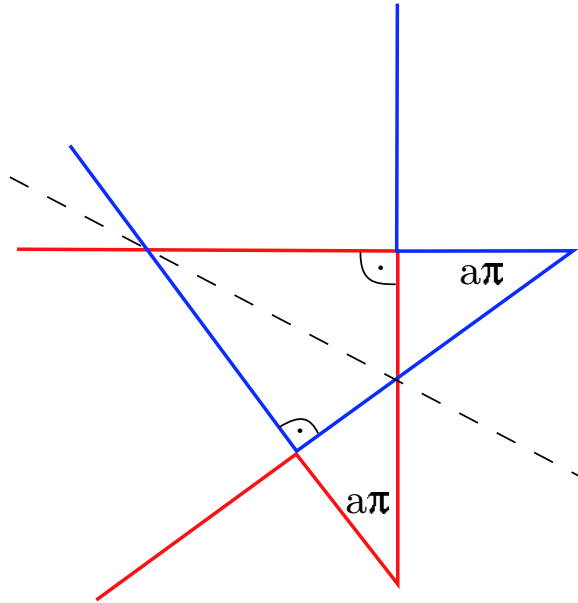

Figure 18: Step 1

Separate the blue and red polygons, and reflect the blue polygon at the x-axes. These polygons form two unbounded quadrilaterals. Label them as indicated.
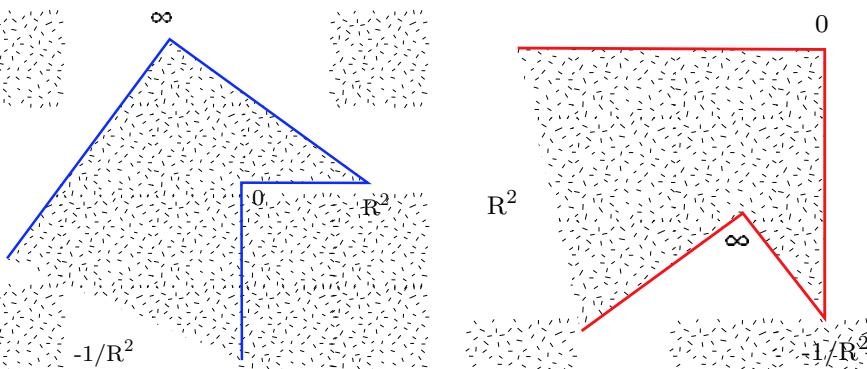

Figure 19: Step 2

Define maps f_1 and f_2 from the upper half plane to the blue and red domains so that labels are mapped to labels. This defines the value of R as a real number.
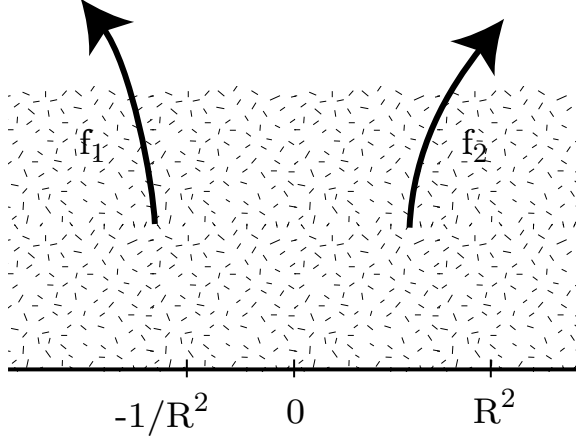
Figure 20: Step 3

If we write

$$Gdh = df_1(z) = f_1'(z)dz$$
$$\frac{1}{G}dh = df_2(z) = f_2'(z)dz$$

then the Schwarz-Christoffel formula implies that

$$Gdh = z^{\frac{1}{2}}\left(R^2 - z\right)^{-1+a}\left(1 + R^2 z\right)^{-1-a}dz$$
$$\frac{1}{G}dh = -z^{-\frac{1}{2}}\left(R^2 - z\right)^{-1-a}\left(1 + R^2 z\right)^{-1+a}dz$$

so that

$$dh = \frac{i}{\left(z - R^2\right)\left(1 + R^2 z\right)}dz$$
$$G(z) = iz^{\frac{1}{2}}\left(\frac{R^2 - z}{1 + R^2 z}\right)^{a}$$

Using the substitution $z = w^2$ gives back the formulas in the beginning, up to irrelevant constant factors.

We need to check that the image domains under the Schwarz-Christoffel maps $\int Gdh$ and $\int 1/Gdh$ are congruent and correctly aligned.

For the correct alignment, observe that the integrand Gdh (resp. $\frac{1}{G}dh$) is positive (resp. negative) in the interval $(0, R^2)$, so that this interval is mapped to horizontal lines with the correct orientation.

For the congruence, we use the map $\iota(z) = -\frac{1}{z}$ of the upper half plane and compute that

$$\iota^* Gdh = z^{-\frac{1}{2}}\left(R^2 - z^{-1}\right)^{-1+a}.$$

38

$$(1 + R^2 z^{-1})^{-1-a} \, z^{-2} \, dz$$
$$= \quad e^{i\theta} \frac{1}{G} dh$$

for some real number θ.

We now check that the period conditions are satisfied. For the vertical periods we use

$$dh = \frac{iw}{(w^2 - R^2)(R^2 w^2 + 1)} dw$$

in the four-punctured sphere to compute with the residue theorem

$$\oint_{\pm R} dh = - \oint_{\pm i/R} dh = - \frac{\pi}{1 + R^4}$$

For the horizontal periods, the symmetry of the constuction proves that the periods of $G dh$ and $\frac{1}{G} dh$ are complex conjugate.

5.7   The Schwarz-Christoffel formula

We will discuss the classical Schwarz-Christoffel formula which was needed in the previous section and which we will need again. This formula is an integral expression for maps from the upper half plane to an arbitrary euclidean polygon bounded by straight lines.

Definition **5.1** *A euclidean polygon is a simply connected region in the plane (or more generally a simply connected Riemann surface with boundary over the plane) such that all boundary components consist of straight lines and segments, meeting in a discrete set of vertices.*

That is, we allow for unbounded polygons but exclude domains with holes or handles.

By the Riemann mapping theorem, there is a biholomorphic map f from the upper half plane to any such euclidean polygon. This map extends continously (but not necessarily injectively) to the real axes. Let us denote the preimages of the vertices by t_i, this will be a discrete subset of the real line.

Denote by α_j the angle of the polygon at $f(t_j)$. Then we have the

39

Theorem **5.1 (Schwarz-Christoffel formula)**

$$f(z) = C_1 + C_2 \int^w \prod_j (z - t_j)^{a_j} dz$$

A proof can be found in [Neh52].

6 Minimal Surfaces Defined On Punctured Tori

We discuss minimal surfaces defined on punctured tori. We recall basic facts from complex variables about complex tori and elliptic functions. For the use of geometrically defined elliptic functions in the context of minimal surfaces, see [HKW93].

6.1 Complex tori

A complex torus is given by a lattice Λ in $\mathbb{C}$, that is, a free abelian subgroup of rank 2 in $\mathbb{R}^2$. Such a subgroup can be written as

$$\Lambda = \{a\omega_1 + b\omega_2 : a, b \in \mathbb{Z}\}$$

Here ω_1 and ω_2 are two complex numbers which are linearly independent over $\mathbb{R}$. They form a basis of the lattice, and the parallelogram spanned by them is called a fundamental parallelogram of the torus.

A meromorphic function $f(z)$ on $\mathbb{C}$ is called elliptic if it is periodic with respect to Λ, that is if

$$f(z + \omega) = f(z) \qquad \forall \omega \in \Lambda$$

Associated to each elliptic function is its divisor

$$(f) = \sum n_j P_j$$

which is a formal linear combination of the zeroes and poles P_j of f in $T = \mathbb{C}/\Lambda$ with their multiplicities n_j.

The degree of a divisor is

$$deg(f) = \sum n_j$$

The existence of meromorphic functions with given divisors is settled by the following important

Theorem 6.1 (Abel) *There is an elliptic function $f(z)$ on a torus $T = \mathbb{C}/\Lambda$ with divisor $\sum n_j P_j$ if and only if*

1. $\sum n_j = 0$

2. $\sum n_j P_j \in \Lambda$

Example **6.1** On any torus, there is a meromorphic function with a double order pole at the corners of the fundamental parallelogram and a double order zero at the center.
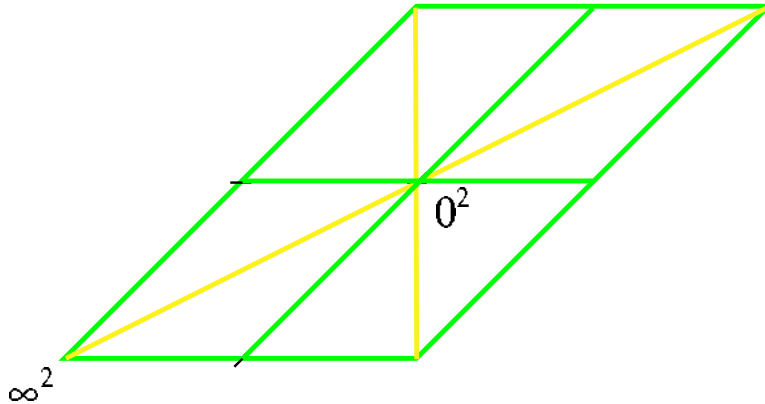

Figure 21: A divisor

6.2   Algebraic equations

Take an elliptic function $p(z)$ with double order pole and double order zero on a torus T. Then $p'(z)$ has a triple order pole and three zeroes, at which p takes the values $0, a, b$. Divisor considerations show that $p(z)$ must satisfy a differential equation

$$p'(z)^2 = c \cdot p(z) \cdot (p(z) - a) \cdot (p(z) - b)$$

We can scale $p(z)$ and the lattice such that

$$p'(z)^2 = p(z)(p(z) - 1)(p(z) - \lambda)$$

The constant λ is called the modular invariant of the torus T.

In principle, every elliptic function on T can be expressed algebraically in terms of $p(z)$ and $p'(z)$. Instead of working with z as a coordinate of T and computing elliptic functions by computing first $p(z)$ and $p'(z)$, we can as well use $v = p(z)$ as a coordinate and compute $w = p'(z)$ using

$$w^2 = v(v - 1)(v - \lambda) \tag{12}$$

This equation can indeed be suitably understood as defining a set of points which is complex isomorphic to T.

Hence: Working with elliptic functions on T is equivalent to working with rational functions in v and w such that 12 holds.

This approach has the advantage that it generalizes easily to higher genus Riemann surfaces. But it is limited insofar as it is not always easy to express a given elliptic function in terms of p and p'.

6.3   Theta functions

On the Riemann sphere, the meromorphic functions are just the rational functions, which are products and fractions of linear functions. It is not quite as simple for meromorphic functions on tori, but we can come close to it if we use theta functions instead of linear functions.

To any lattice, spanned by 1 and τ, we associate an entire function $\theta(z; \tau)$:

$$\theta(z; \tau) = \sum_{n=-\infty}^{\infty} e^{\pi i (n+1/2)^2 \tau + 2\pi i (n+1/2)(z+1/2)}$$

This complicated looking expression has the advantage that it converges rapidly. Here are the important properties of θ:

$$\begin{aligned}
\theta(0; \tau) &= 0 \quad \text{(simple zero)} \\
\theta(z+1; \tau) &= -\theta(z; \tau) \\
\theta(z+\tau; \tau) &= e^{2\pi i (z+\frac{\tau+1}{2})} \theta(z; \tau)
\end{aligned}$$

In the following, we will omit the second argument τ. In a fundamental parallelogram, $\theta(z)$ has no further zeroes, and this allows the construction of meromorphic functions with given transformation laws with respect to the lattice periods:

Lemma 6.1 *Let $a_i, b_i \in \mathbb{C}, i = 1 \ldots n$. Then*

$$f(z) = \prod_{i=1}^{n} \frac{\theta(z - a_i)^{\alpha_i}}{\theta(z - b_i)^{\beta_i}}$$

has simple zeroes at a_i, simple poles at b_i and satisfies

$$\begin{aligned}
f(z+1) &= (-1)^{\sum \alpha_i - \beta_i} f(z) \\
f(z+\tau) &= e^{2\pi i \sum \alpha_i a_i - \beta_i b_i} f(z)
\end{aligned}$$

Exercise 6.2 *Use this to prove the existence part of Abel's theorem!*

6.4 Elliptic functions via Schwarz-Christoffel maps

Any conformal torus can be specified by taking a parallelogram in the euclidean plane and identifying opposite edges. This torus comes with a flat metric which also defines the conformal structure. It will be helpful to think of this flat metric as a special *flat geometric structure* in the sense that it can be given by local coordinate charts into the euclidean plane $\mathbb{E}$ (which are the identity maps on open subsets of the interior of the parallelogram) so that the change of coordinate maps are just translations.

On the other hand, given such a geometric structure, the exterior derivatives of the coordinate charts fit together to define a globally well-defined holomorphic (with respect to the inherited conformal structure) 1-form on the torus. In our example, this is just the 1-form dz inherited from the euclidean plane. It is worth noting that the periods of this 1-form are *visible* in the geometry of the flat structure, namely as the edge vectors of the parallelogram.

We will now repeat this construction in a slightly more complicated situation. Take again a parallelogram in the euclidean plane, but now remove it from the plane and identify again opposite edges from the remainder (figure 22).
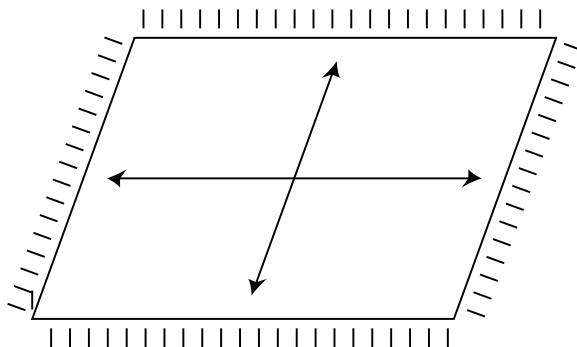
Figure 22: Cone metric construction of meromorphic 1-forms

Topologically, we get a punctured torus, with the puncture corresponding to the point ∞ of the extended plane. Again this torus carries a flat geometric structure of the same type as before, but this time with two singular points: One corresponds to the point ∞ in the euclidean plane, the other to the vertices of the parallelogram which are identified to a single conical point with cone angle 6π. Away from these singularities, this flat structure defines again a holomorphic 1-form on the torus by taking the exterior derivative of local charts.

To analyze the behavior at the singular points, we first look at a neighborhood of ∞. Here the geometry is precisely the same as for dz at ∞ in the euclidean plane, which has a double order pole there. Hence our holomorphic 1-form extends meromorphically to ∞ with a double order pole. The singularity at the other singular point (the parallelogram vertex) is removable, as the exterior derivative of coordinate function nearby is bounded. Hence the 1-form also extends to this point, and by the residue theorem, it has a double-order zero there. In fact, in the next section we will see that a cone angle α leads to a zero of order $\frac{\alpha}{2\pi} - 1$.

The periods of this 1-form are again easy to read off as the parallelogram edges. To avoid confusion: The parallelogram torus is in general *not* the same conformal torus as the 'removed parallelogram torus'. A notable exception is the square torus.

At first glance, surprisingly, this family of 'removed parallelogram tori' does not exhaust the set of tori with meromorphic 1-form with double order pole and zero. Firstly, the parallelogram can degenerate without the torus degenerating!
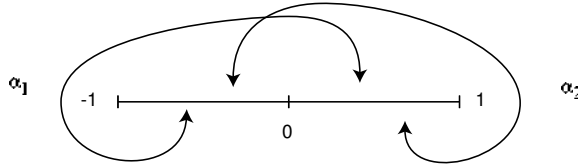

Figure 23: A rhombic torus with real periods

To see this, take once again the euclidean plane and slit it along the interval $[-1, 1]$. Choose a number $a \in [0, 1)$ and glue the $[-1, -a]$ portion of the upper (resp. lower) part of the slit to the $[a, 1]$ portion of the lower (resp. upper) part of the slit.

In figure 23, we have indicated this for $a = 0$. This identification gives again a flat torus with two singular points with the same cone angles as before. The periods of the corresponding 1-form are now both real, namely $-a$ and $1 - a$. Within this 1-parameter family there is precisely one rhombic torus, corresponding to $a = 0$: In this case, the reflections about the real and imaginary axes are well defined on the torus, and have a connected fixed point set each, which implies rhombicity.

For rectangular tori, this construction can be understood more concretely in terms of Schwarz-Christoffel maps. The complement of a rectangle in the plane is the image domain of a fundamental rectangle under a map $\int^z p(z)dz$, where $p(z)$ is an elliptic function with double order pole and double

order zero in the torus. If we use the reflectional symmetries of the rectangle to decompose the rectangle into four congruent smaller rectangles half the size of the original rectangle, each of these smaller rectangles will be mapped by $\int^z p(z)dz$ to a quarter of the complement-of-the-rectangle-domain. Now both domains, the small rectangle and the complementary quarter, are euclidean polygons which are images of the same upper half plane under two Schwarz-Christoffel maps: The rectangle is obtained using

$$\int^p u^{-\frac{1}{2}}(u-1)^{-\frac{1}{2}}(u-\lambda)^{-\frac{1}{2}}du$$

and the complementary quarter is given by

$$\int^p u^{+\frac{1}{2}}(u-1)^{-\frac{1}{2}}(u-\lambda)^{-\frac{1}{2}}du$$

Here λ is the modulus of the torus (or rectangle), it is a negative real number. If we use $u = p(z)$ as a torus coordinate, the identity map on the torus can be rewritten as

$$
\begin{aligned}
z &= \int^z 1dz \\
&= \int^p \frac{1}{p'(z)}du \\
&= \int^p \frac{1}{\sqrt{u(u-1)(u-\lambda)}}du
\end{aligned}
$$

and similarly, the map to the exterior of the rectangle can be rewritten as

$$
\begin{aligned}
\int^z p(z)dz &= \int^p \frac{p(z)}{p'(z)}du \\
&= \int^p \frac{\sqrt{u}}{\sqrt{(u-1)(u-\lambda)}}du
\end{aligned}
$$

This suggests that the function p, which we have just abused as a coordinate function, maps the quarter-rectangle conformally to the upper half plane. One can prove this easily by studying its boundary behavior or using the above computations.

It makes it in fact possible to define $p(z)$ by this property, see [HKW93].
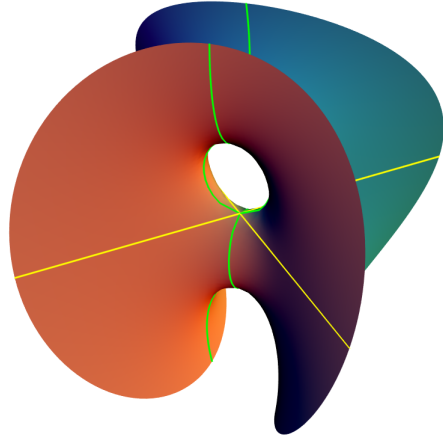
6.5 The Chen-Gackstatter surface

Figure 24: The Chen-Gackstatter surface

The Chen-Gackstatter surface was the first complete minimal surface of finite total curvature defined on a torus. It has the same symmetries as the Enneper surface, which implies that the only possible torus it can live on is the square torus. It has just one end of Enneper type at which the Gauss map can be assumed to have a simple zero and the height differential a triple order pole. We can put the puncture representing the end at the lower left corner of the fundamental square. The straight lines on the surface become the diagonals of the square and the planar symmetry lines become the edge bisectors and boundary edges. They intersect on the surface in the end at infinity and in the three points with vertical normal, and on the square at the four halfperiod points. This determines the divisor of G and dh as follows:
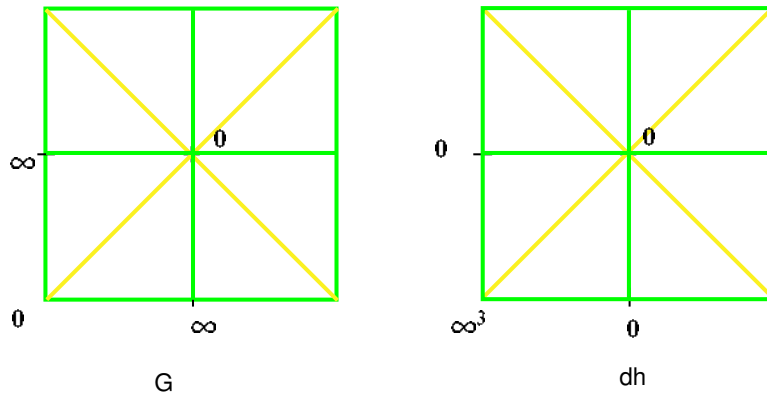

Figure 25: Divisors of the Weierstrass data

This suggests that we use the algebraic description, as both dh and G are easily expressible in terms of w and v:

The underlying torus T is the square torus, which is given by the algebraic equation

$$w^2 = v(v-1)(v+1)$$

The Gauss map G and height differential dh are given by

$$
\begin{aligned}
G &= \rho v/w \\
dh &= dv
\end{aligned}
$$

where ρ can be explicitly determined as $\rho = \frac{\Gamma(\frac{1}{4})}{\sqrt{6}\Gamma(\frac{3}{4})}$ to satisfy the horizontal period condition.

Mathematica Notebook **6.2** The notebook *ChenGackstatter.nb* integrates the Weierstraß data for the Chen-Gackstatter surface in terms of hypergeometric functions, computes the López-Ros parameter and plots the surface.

If we restrict our attention to the quarter of the surface which is given by the upper v-plane (which is the piece of the surface one gets if one cuts it apart by the vertical coordinate planes), the complex coordinate maps can be expressed as Schwarz-Christoffel maps:

$$
\begin{aligned}
\int^p G\,dh &= \int^p v^{\frac{1}{2}}(v-1)^{-\frac{1}{2}}(v+1)^{-\frac{1}{2}}dv \\
\int^p \frac{1}{G}dh &= \int^p v^{-\frac{1}{2}}(v-1)^{\frac{1}{2}}(v+1)^{\frac{1}{2}}dv
\end{aligned}
$$

so that these two maps map the upper half plane to domains which are complementary regions.

For the uniqueness of this surface, see [Lop92, Web99].

6.6   Riemann's minimal surface

Riemann's minimal surface is a singly periodic surface invariant under a translation in space.
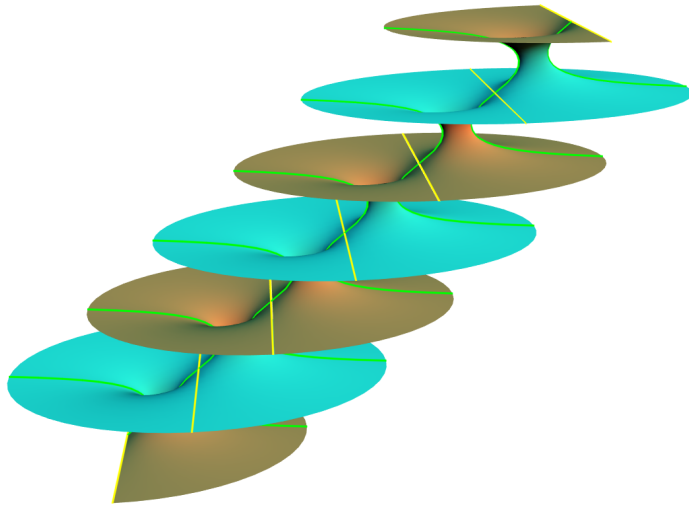
Figure 26: Riemann's minimal surface

The quotient of the surface by its translational symmetry group is a torus with two ends. We arrange the surface in space so that the Gauss map is infinite at one end and zero at the other. The ends are planar, so the height differential will be regular there. As there are no further ends, the height differential must be holomorphic, hence a constant multiple of dz. This means that the Gauss map is nowhere else vertical.

The symmetries imply that the underlying torus is rectangular.

Figure 27: Divisor of the Gauss map

The vertical period condition requires only that one of the two period is imaginary, which is the case for dz. Also, the horizontal period condition needs only to be satisfied for one period. If we normalize $G(z) = \rho p(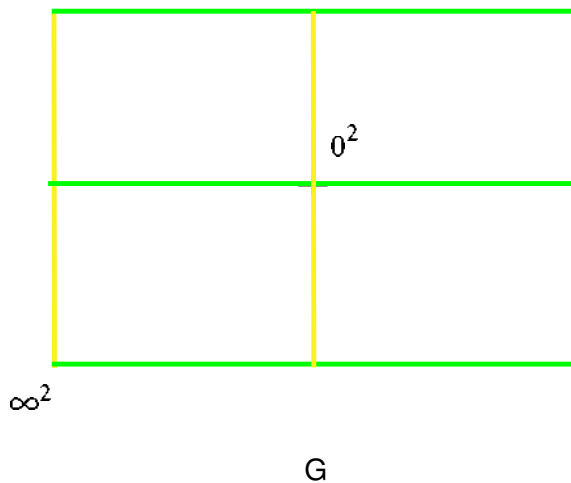z)$ such that $G(z)$ becomes a translation of $1/G(z)$ by $(1 + \tau)/2$, Gdh and $1/Gdh$ have the same periods. As for one cycle these are real, they are also complex conjugate.

A striking property of Riemann's minimal surfaces is that they are foliated horizontally by circles (or, at the level of the ends, by straight lines). See [MPR98].

6.7   The fence of Catenoids

The fence of catenoids illustrates what happens if one wants to add a handle to the catenoid. A theorem of R. Schoen [Sch83] implies that this is not possible. However, one is allowed to try.
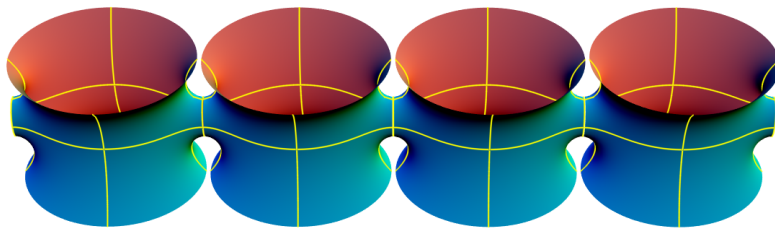
Figure 28: A fence of catenoids

Let's suppose we have a catenoid with an additional horizontal handle. As a finite total curvature surface, this would be represented by a twice punctured torus. Let us assume that the surface is symmetric with respect to reflections at the coordinate planes. This implies that the torus is rectangular, and the planar symmetry lines are represented by the horizontal and vertical symmetry lines of a fundamental rectangle. All special points are placed at the intersections of these points. At the catenoid ends, the Gauss map has a simple pole and zero, and the same holds for the two points on the handle where the Gauss map is vertical. On the other hand, the height differential must have simple poles at the catenoid ends with real residues, and simple zeroes at the two handle points to compensate for the Gauss map. In terms of our elliptic function p, the height differential can thus be

Figure 29: A catenoid with an attempted handle

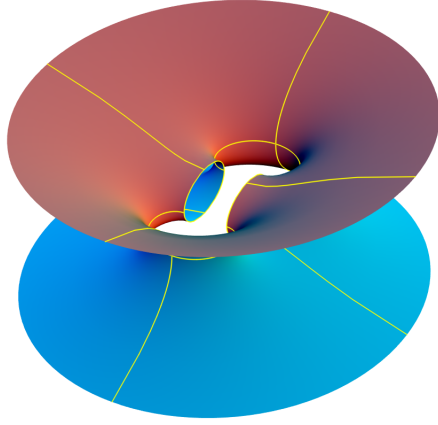written as dp/p (up to an irrelevant real scale factor). It remains to deal with the horizontal period condition. We see that $G(z)dh = \rho p(z)dz$ and $\frac{1}{G(z)}dh = \frac{1}{\rho p(z)}dz$.

Up to a scalar factor c, these two forms are translates of each other, hence for all cycles γ

$$\int_\gamma \frac{1}{G}dh = c\int_\gamma Gdh$$

We can solve the horizontal period problem for one cycle α easily by adjusting the Lopez-Ros parameter ρ. We can also rotate the surface in space so that both periods of Gdh and $\frac{1}{G}dh$ over α become real. Then the above equation implies that (in this normalization) we have $c = 1$. Hence all periods of Gdh and $\frac{1}{G}dh$ must be real. However, this is impossible on a rectangular torus. This follows for instance from the Legendre relation for the periods of dz and pdz:

$$\omega_1\pi_2 - \omega_2\pi_1 = 8\pi i$$

as $\omega_2 = i\omega_1$. So we are forced to leave one horizontal period unclosed. This leads to a 1-parameter family of simply periodic minimal surfaces which depends on the modulus of the rectangular torus. Depending on this parameter, the handle grows inwards as below or outwards as above.
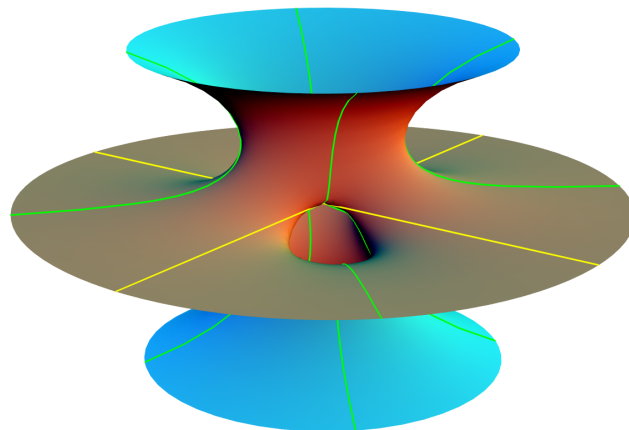
51

6.8   Costa's minimal surface

Figure 30: The Costa surface

The Costa surface was the first embedded minimal torus ([Cos82, Cos84]. It lives on the square torus with three punctures, has total absolute curvature $\kappa = 12\pi$, two catenoid ends and one planar end. Later the planar end was shown to be deformable into a catenoid end, giving rise to a 3-ended embedded minimal surface for each rectangular torus.

There are also two straight line on the surface which pass through the origin.

Assuming the existence of such a surface, we derive its Weierstraß representation as follows:

We arrange the surface so that the Gauss map is vertical at the ends.

At the two catenoid ends, dh must have simple poles with real residue. Here the Gauss map has two simple poles. At all other points, dh must be regular. Hence we expect two more zeroes. One of them will be at the origin where the two straight lines meet, and here the Gauss map must also have a pole.

For the second zero of dh, we have two choices, forced by symmetry: Either we put it at the planar end, or we make the zero at the origin a double zero. In the latter case, the Gauss map must also have a double pole at the origin to make the metric regular there. But then Gauss map would have a fourth order zero at the planar end and dh would be regular, contradicting the quadratic growth of the metric at planar ends. Hence we expect the

second zero of dh at the planar end. This must then be compensated by a triple order zero of the Gauss map.
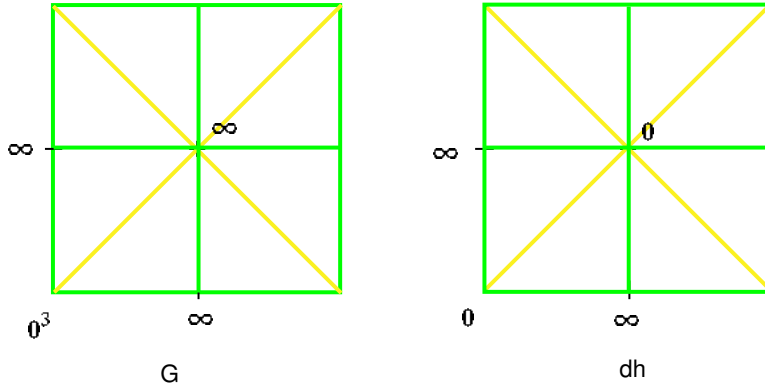

Figure 31: Divisors for the Costa surface

Again, the surface is defined on the square torus $w^2 = v(v^2 - 1)$. The point $(v, w) = (\infty, \infty)$ represents the planar end, the points $(v, w) = (\pm 1, 0)$ the catenoid ends, and $(0, 0)$ the origin. We can express the Weierstrass data in terms of v and w as follows:

$$
\begin{aligned}
G &= \rho/w \\
dh &= \frac{\lambda dv}{(1 - v^2)w}
\end{aligned}
$$

The free parameters are determined to kill the periods. First, the height differential must have real residues at the ends, hence λ must be real, and we can choose it to be 1 by scaling the surface. To determine ρ, we would like to evaluate two period integrals. Let α be a horizontal cycle on the torus. This becomes a closed curve γ^* encircling 0 and 1 on the v-sphere, and we can evaluate

$$
\begin{aligned}
\int_{\gamma^*} \frac{1}{G} dh &= \frac{2}{\rho} \int_0^1 \sqrt{\frac{v}{1 - v^2}} \, dv \\
&= \frac{4\sqrt{\pi}\,\Gamma(\frac{3}{4})}{\rho \Gamma(\frac{1}{4})}
\end{aligned}
$$

Unfortunately, it is not possible to evaluate $\int_{\gamma^*} \frac{1}{G} dh$ this way, because the integrand has a too bad singularity at $(v, w) = (1, 0)$. To circumvent this problem, we introduce a technique which is important both for theoretical and practical purposes: We replace the 1-form $1/Gdh$ by one with harmless singularities, using partial integration. First differentiating the surface equation $w^2 = v(v^2 - 1)$ gives

$$
2wdw = (3v^2 - 1)dv
$$

53

and hence

$$
\begin{aligned}
d\frac{v}{w} &= \frac{w\,dv - v\,dw}{w^2} \\
&= \frac{dv}{w} - v\frac{3v^2 - 1}{2w^3}dv \\
&= \frac{dv}{w} - \frac{3v(v^2 - 1) + 2v}{2w^3}dv \\
&= -\frac{dv}{2w} - \frac{v}{v(v^2 - 1)w}dv \\
&= -\frac{dv}{2w} - \frac{dv}{(v^2 - 1)w}
\end{aligned}
$$

so that

$$
\begin{aligned}
\int_{\gamma^*} Gdh &= -2\rho \int_0^1 \frac{dv}{2w} \\
&= \frac{2\sqrt{\pi}\,\Gamma(\frac{5}{4})}{\Gamma(\frac{3}{4})}
\end{aligned}
$$

and we can determine ρ. The other period which needs to be killed is along the vertical torus cycle, or the cycle encircling 0 and -1 in the v-plane. Because of the symmetries of the construction, however, this period is automatically killed together with the γ-period.

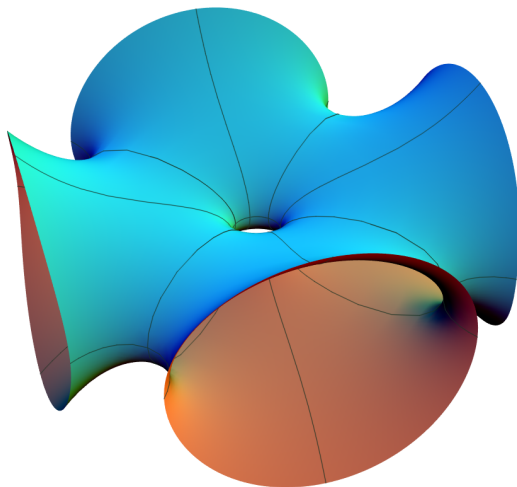## 6.9 The Jorge-Meeks k-noids with an additional handle

Figure 32: A 4-noid with handle

The k-noids of Jorge and Meeks are complete minimal surfaces of finite total curvature defined on the sphere with catenoid ends at the punctures corresponding to the kth roots of unity. It is possible to add a handle 'connecting' the two symmetry points. This has been observed by Karcher (see remark 5.5 on page 113 in [Kar88] and the diploma thesis [Ste96], where the existence is shown using a conjugate Plateau construction).

The underlying Riemann surface of these k-noids is a torus spanned by 1 and $k \cdot \tau$, punctured at k points. The reflectional symmetries imply that the torus is rectangular. The rotational symmetry of the surface becomes a conformal automorphism rotating the punctures, hence we can assume the punctures to be at the points $j/k\tau$, $\quad j = 0 \ldots k - 1$. Denote by T' the quotient torus spanned by 1 and τ. While the height differential is invariant under the rotation and hence descends to T', the Gauß map becomes a multivalued function satisfying

$$
\begin{aligned}
G(z + 1) &= G(z) \\
G(z + \tau) &= \zeta G(z)
\end{aligned}
$$

with ζ a kth root of unity. We can construct G using theta-functions. Take

$$
\begin{aligned}
G(z) &= \rho \frac{\theta(z - n^-)}{\theta(z - n^+)} \\
dh &= \frac{\theta(z - n^+)\theta(z - n^-)}{\theta(z)\theta(z - (\tau + 1))} dz
\end{aligned}
$$

From lemma 6.1 and the assumed periodicity we deduce from $n^{\pm} = \frac{1+\tau}{2} \mp \delta_0$ that $2\delta_0 = n^- - n^+ = \frac{k-1}{k}$ so that $\delta_0 = \frac{k-1}{2k}$.

This determines the divisor of dh completely. With these constructions conditions (1) and (2) are satisfied, and we are left with the period condition for dh, which we won't discuss there.

Mathematica Notebook 6.3 However, there is a Mathematica notebook *(k-noidsg=1).nb* available where the period problem is solved numerically, using theta functions.

In the same way as the ordinary k-noids are limits of singly periodic Scherk surfaces, the k-noids with a handle are limits of singly periodic Scherk surfaces with handles.
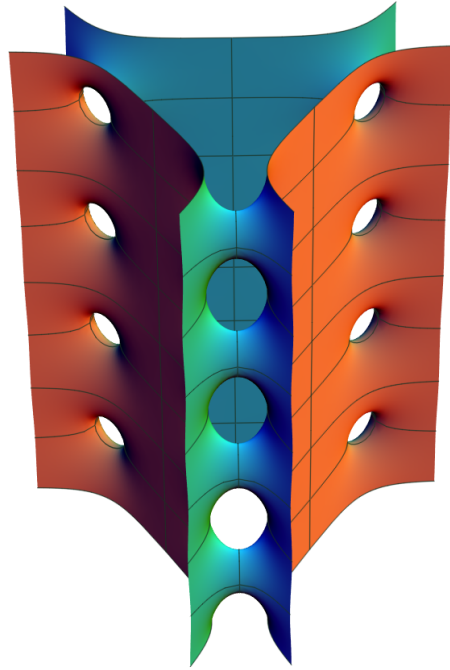
Figure 33: A singly periodic Scherk surface with six ends and vertical handles

6.10 Parameterizing minimal surfaces

This subsection explains how to find good parameter lines on a minimal surface. This is important, as such parameter lines often help to understand the geometry of the surface. It also yields very attractive surface models.

Given the Weierstraß representation of a surface, we have a conformal parameterization for free. So why not use the standard coordinate lines on the parameter domain? As an example, look at Costa's surface. It is clearly sufficient to draw a fundamental piece of the surface with respect to its eightfold symmetry. Such a piece is parameterized by the first quadrant. Recall that the origin is mapped to the origin in $\mathbb{R}^3$, the positive imaginary axes is mapped to a straight halfline, the segment $(0, 1)$ is mapped to a planar symmetry curve which connects the origin with the top catenoid end and the segment $(1, \infty)$ is another planar symmetry curve connecting the planar end with the catenoid end.

The obvious drawback of using a rectangular coordinate grid in the first quadrant is that it is not adapted at all to the planar and the catenoid ends. In our discussion of the minimal surfaces defined on the plane or the punctured plane we have seen that the ends of a minimal surface are quite well

treated by using polar coordinates centered at the punctures which represent the ends.

For our parameterization of the Costa patch, we can deal with the planar end this way by using planar coordinates in the first quadrant. This however neglects the catenoid end.

Our ultimate source domain will be the parallel strip $\mathbb{R} \times (0, \pi)$. This can be mapped (conformally) to the first quadrant such that $-\infty$ is mapped to 1 and $+\infty$ is mapped to ∞. In fact, such a map is explicitly given by

$$u \mapsto \sqrt{1 + e^u}$$

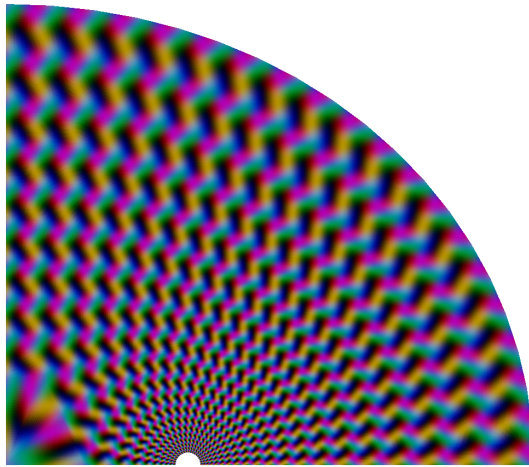Figure 34: Coordinate mesh in the first quadrant

This explicit approach works fairly well if the parameter domain of a fundamental piece of the surface is sufficiently simple so that a mapping function from a standard domain to it can be found, and so that the ends of the surface are represented by at most two boundary points of the domain. This is the case for many (though not all) of the known minimal surfaces.

7 Higher Genus Minimal Surfaces

We discuss how minimal surfaces of higher genus can be described and how one can solve the period problem numerically. For background about Riemann surfaces, see [FK80, Gun66].

7.1 Riemann surfaces

Riemann surfaces are 2-dimensional manifolds which are given by an atlas of coordinate charts into $\mathbb{C}$ so that the change-of-coordinate maps are holomorphic. A convenient way to define Riemann surfaces is by specifying algebraic relations between meromorphic functions. This will also allow us to write down meromorphic functions and 1-forms on the Riemann surface in an explicit way. Here is an example.

Example 7.1 Consider the subset

$$X_0 = \{(x, y) \in \hat{\mathbb{C}} \times \hat{\mathbb{C}} : y^2 = x^6 - 1\}$$

There is a natural way to turn this into a compact Riemann surface. This requires to think carefully about points at ∞, but we will largely ignore this. The coordinate functions x and y become meromorphic functions on this surface, and all meromorphic functions can be expressed rationally in x and y.

Another way of realizing this example quite concretely is the following: Take two copies of the Riemann sphere, punctured at the sixth roots of unity (the zeroes of $x^6 - 1$). Define $f(z) = z$ on these two copies. When computing the square root $g(z) = \sqrt{f(z)^6 - 1}$ on one of these copies, we face a problem near the roots of unity: Analytic continuation of g along a loop around one of these points results in a sign change of g. So we can't define g globally on just one of these copies. The idea is now to glue the two copies together suitably so that whenever we continue g analytically around one of the punctures, we switch to the other copy. To do this more formally, we first restrict g to a subdomain of the punctured sphere on which we can define g globally. There are several choices for such domains: An efficient choice is to connect the six punctures in pairs by disjoint paths and then to slit the plane along these paths. Continuation of $g(z)$ around such a cut forces a double sign change of the square root so that g becomes well defined. Another choice of a suitable subdomain applies under more general circumstances: Slit the plane along cuts which emanate from the six punctures radially to infinity. Then this is a simply connected domain, there is a priori no continuation conflict. It

turns out that the surface we are going to construct will be independent of the choice of cuts we make, so we will continue with the second construction.

Now take the two copies of the slit Riemann sphere and define $g(z)$ on both of them, albeit with different sign. Glue the two copies together by gluing them along the slits crosswise. This purely topological construction ensures that the functions f and g become continuous on the glued topological surface. However, it is easy to make this topological surface into a Riemann surface so that f and g become meromorphic functions: Away from the cuts, we take the identity map to the Riemann sphere as coordinates. On the cuts coordinate maps are given also by the identity maps of the two different spheres which are used for the gluing. Along the slit, these maps take the same values by construction. At the punctures, it takes a little work to to construct a local coordinate which is holomorphically compatible with the other charts. Let's look at the puncture at 1. The idea is to use the function $\sqrt{z-1}$ as a local coordinate here. While this is impossible on just one copy of $\hat{\mathbb{C}}$, the two glued copies make $\sqrt{z-1}$ single-valued in a neighborhood of 1. The change of coordinate maps will be holomorphic, as $\sqrt{z-1}$ is holomorphic in neighborhoods of points away from 1. Note that we don't need to worry about holomorphicity at 1, as this point isn't covered by any other coordinate. A final issue arises with the point ∞ (to which all the slits connect). As we have an even number of slits, the square root function does not change its sign here, so on the Riemann surface we construct there are actually two points ∞ coming from the two different Riemann spheres.

7.2 Differential forms

Let's suppose we are given a Riemann surface X by an algebraic equation. For simplicity on concreteness, we assume that the equation has the form

$$y^n = P(x)$$

where P is a polynomial of degree m. Then x will be a meromorphic function of degree n on X which has zeroes precisely at the copies of the points $(0, y_j)$ with $y_j^n = P(0)$.

We will now use the functions x and y to write down meromorphic differential forms on a Riemann surface.

Example 7.2 Let X given by

$$y^2 = P(x) = x^6 - 1$$

Denote the two zeroes $(0, \pm\sqrt{-1})$ by $0_{1,2}$ and the two copies of ∞ by $\infty_{1,2}$. Then x has simple zeroes at $0_{1,2}$ and simple poles at $\infty_{1,2}$. The function y has simple zeroes at the six zeroes $x_{1...6}$ of $P(x)$ and triple order poles at $\infty_{1,2}$. This is consistent with the important fact that the number of zeroes of a meromorphic function on a compact Riemann surface must be equal to the number of its poles, counted with multiplicity.

We obtain meromorphic differential forms on X by taking exterior derivatives of meromorphic functions and and multiplying them by other meromorphic functions. For instance, dx will have two double order poles at $\infty_{1,2}$ and simple zeroes at $p_{1...6}$. Differentiating the surface equation gives

$$ydy = 3x^5 dx$$

and from this we can compute that dy has fifth order zeroes at $0_{1,2}$ and fourth order poles at $\infty_{1,2}$. We also see that the forms $\frac{dx}{y}$ and $x\frac{dx}{y}$ are holomorphic on the surface.

Here are these data in a tabular form:

	$0_{1,2}$	$\infty_{1,2}$	$x_{1...6}$
x	0^1	∞^1	$*$
y	$*$	∞^3	0^1
dx	$*$	∞^2	0^1
dy	0^5	∞^4	$*$
dx/y	$*$	0^1	$*$
xdx/y	0^1	$*$	$*$

Example 7.3 Consider now the Riemann surface given by

$$y^2 = P(x) = x(x^6 - 1)$$

In this case, there is only one copy of 0 in the surface (denoted by 0) and also only one copy of ∞.

Thus x has a double zero at 0 and a double order pole at ∞. Again, the behavior of y can be read off from the equation: It has simple zeroes at the seven zeroes $x_{1...7}$ of P and a seventh order pole at ∞, due to the branching at ∞.

This time, dx will have a triple order pole at ∞ and simple zeroes at $x_{1...7}$. We could again compute the data for dy by differentiating the surface equation. We also see that the forms $\frac{dx}{y}, x\frac{dx}{y}$ and $x^2\frac{dx}{y}$ are holomorphic on the surface.

We introduce a bit of notation which we have already used for tori:

Definition 7.1 *Let f be a meromorphic function on a Riemann surface. Let p_i be the set of zeroes and poles of f and n_i their multiplicities. Then the formal linear combination*

$$(f) = \sum n_i p_i$$

is called the divisor of f. A similar definition holds for meromorphic 1-forms. The number $\sum n_i$ is called the degree of the divisor/function/form.

Remark 7.4 There is a form of Abel's theorem for Riemann surfaces of arbitrary genus which involves the Jacobian of the Riemann surface.

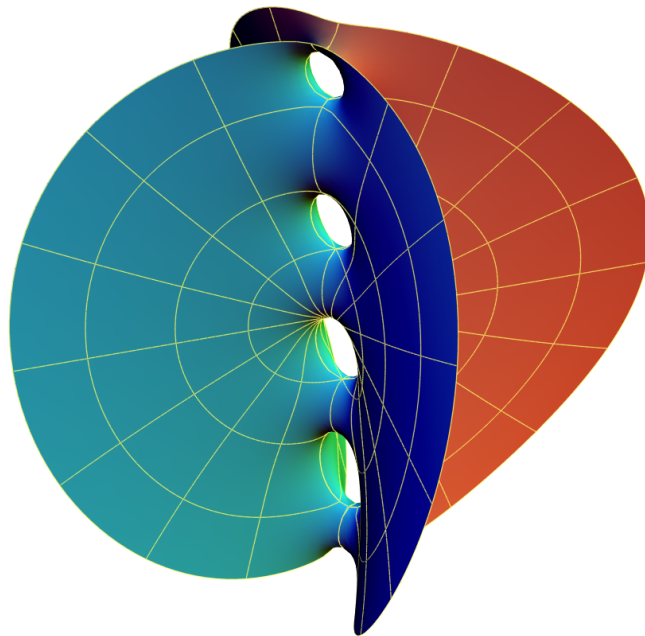## 7.3 The Chen-Gackstatter surface of genus 4

Figure 35: The Chen-Gackstatter surface with four handles

For each genus, there exists a minimal surface of genus g with one Enneper end and the same symmetries as the Enneper surface. These surfaces were first discussed numerically by Thayer and their existence was proven by [Sat96] and [WW98]. They are particularly simple to deal with numerically.

They are defined on Riemann surfaces of genus g, given by

$$y^2 = x \frac{\prod_{j=1}^{g/2} \left(x^2 - a_j^2 \right)}{\prod_{j=1}^{(g+1)/2} \left(x^2 - b_j^2 \right)}$$

with certain numbers

$$1 = a_1 < b_1 < a_2 < b_2 < \ldots$$

The $2g + 2$ points $0, \infty, \pm a_j, \pm b_j$ are all branched points, hence have only single copies on the surface.

The Weierstraß data are given by

$$\begin{aligned} G(x) &= \rho y \\ dh &= dx \end{aligned}$$

The height differential dh has a double order pole at ∞ and the Gauss map a single order pole or zero, depending on the parity of g. Hence ∞ represents an Enneper end, and there are no further ends.

The g free parameters a_j, b_j, ρ are needed to solve the horizontal period problem. While dh is exact, there are $2g$ cycles whose horizontal period conditions must be satisfied. But because of the imposed symmetry, only half of the conditions need to be checked. A suitable choice of these cycles is given by curves encircling the g intervals

$$(0, a_1 = 1), (a_1, b_1), (b_1, a_2), \ldots$$

The evaluation of these integrals can be carried out on the real axes, as the singularities of the integrands at the a_i and b_i are integrable.

If one wants to draw one of these surfaces, one first has to solve the period problem numerically. This requires to solve a g-dimensional nonlinear system of equations, for which the function evaluations are very expensive, as they involve the numerical integration of the periods.

The period problem for these surfaces can be restated in a geometrical way by looking at the following maps from the upper half plane to the complex plane given by

$$\begin{aligned} z &\mapsto \int^z G dh \\ z &\mapsto \int^z \frac{1}{G} dh \end{aligned}$$

It is a surprising but easy to prove fact that the image domains of the upper half plane under these maps are staircase shaped domains which look as follows:
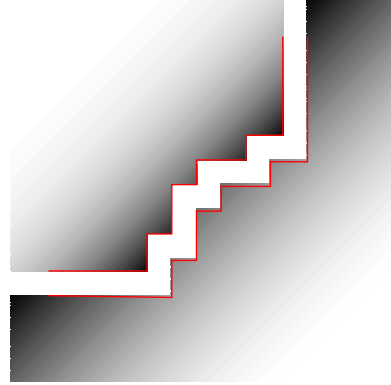
Figure 36: Image domains of the complex coordinate maps

The horizontal period condition is now equivalent to the requirement that these two domains fit together.

These two domains are conformal images of the upper half plane, where the vertices correspond to 0, the $\pm a_i$, and the $\pm b_i$. This suggests another way of constructing minimal surfaces of higher genus: One defines 1-forms Gdh and $1/Gdh$ by specifying the image domains of their integrals, and using the Riemann mapping theorem. The horizontal period condition becomes a geometric condition on the shapes of the domains which needs to be solved under the assumption that the domains of Gdh and $1/Gdh$ are conformal.

7.4   The doubly periodic Scherk surface with handles

It is possible to add handles between each other vertical pair of ends of Scherk's doubly periodic surface. The genus one version of this was constructed by H. Karcher (see [HKW93]).
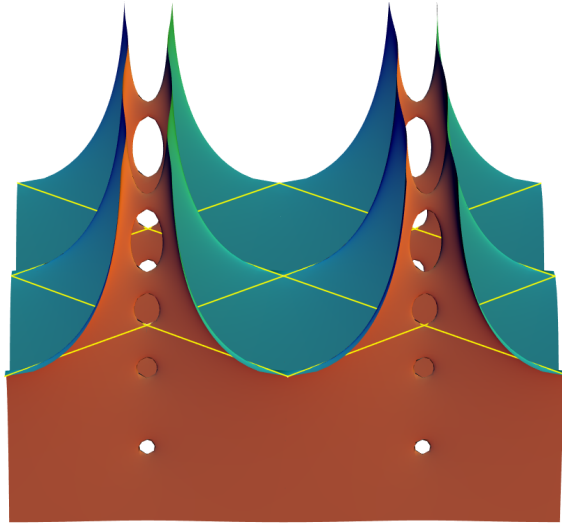
Figure 37: The doubly periodic Scherk surface with four handles

For these surfaces, we use the perspective from the end of the last example. Instead of algebraically defining Riemann surfaces, we define Gdh and $\frac{1}{G}dh$ by the image domains of their integrals:
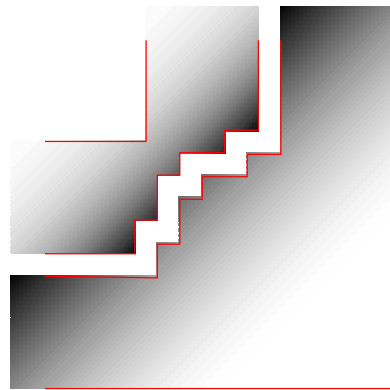

Figure 38: The image domains of the complex coordinates maps for the doubly periodic Scherk surface with four handles

Again, the requirements on these two domains are that they fit together and that they are conformal by a vertex preserving map. Then, these domains are images of a fundamental piece of the doubly periodic Scherk surface with four handles under the maps $\int Gdh$ and $\int \frac{1}{G}dh$.

Observe that the image domains can be obtained from the image do-

mains of the classical Scherk surface by cutting corners along one boundary arc. This process of cutting corners in euclidean domains corresponds to adding handles to the minimal surface.

To obtain explicit formulas for Gdh and $\frac{1}{G}dh$, one expresses these forms as Schwarz-Christoffel integrands for maps to these polygonal domains. These integrands have free parameters which need to be determined numerically so that the domains fit together.

7.5 The generalized Callahan-Hoffman-Meeks surfaces

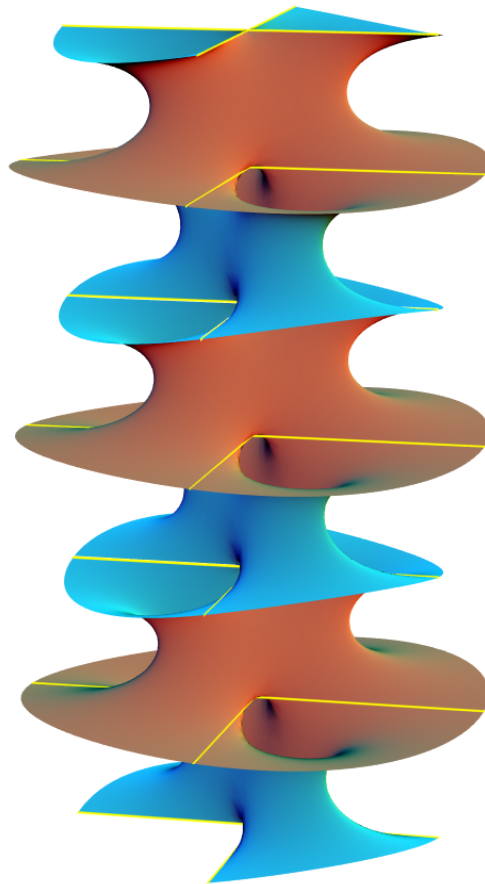The Callahan-Hoffan-Meeks surface is a singly-periodic mutant of the Costa surface:

Figure 39: The Callahan-Hoffman-Meeks surface

Its quotient under a vertical translation is a genus 3 surface, punctured at two points:

$$y^4 = P(x) = x^2(x^2 - 1)(x^2 - a^2).$$

Furthermore, the Weierstraß data are given by

$$Gdh = \frac{1}{x^2 - a^2}\frac{dx}{y}$$

$$\frac{1}{G}dh = \frac{ydx}{x^2 - 1}$$

7.6   Period computations

It is possible to add arbitrarily many handles to each translational funda-mental piece of this surface ([Web00]). Here is an example with two more handles between two consecutive parallel ends:
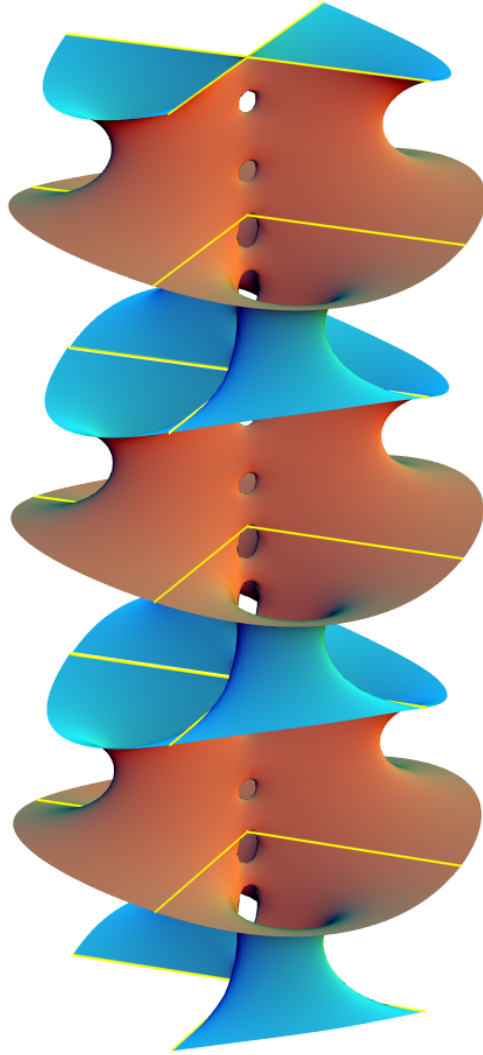
Figure 40: The Callahan-Hoffman-Meeks surface with two more handles

This example is denoted by CHM_3. We will now explain how one can solve the period problem for surfaces of this kind. Even though the method will be quite general, we will use the CHM_1-surface as the main example as here all computations can be carried out by hand.

For solving the period problem of the CHM_1-surface, we have to integrate

$$Gdh = \frac{1}{x^2 - a^2} \frac{dx}{y}$$

over closed cycles on the Riemann surface (the other Weierstraß 1-forms do not cause difficulties). These cycles are represented by closed curves in the x-plane encircling the punctures $0, \pm 1, \pm a$.

This is difficult, because

- The integrand Gdh is multivalued in x

- The integration path is a curve in the complex plane

While it is tempting to replace these integrals by a real line integral between the punctures $-a, -1, 0, 1, a$, this is impossible for the integrals encircling a, as the integrand has a non-integrable singularity there. We have encountered this kind of problem before with Costa's surface.

The idea here is to replace the 1-forms above by cohomologous ones with integrable singularities. For this, one has to find the replacements efficiently.

We discuss this in a slightly more general way: Suppose that a Riemann surface X is given by

$$y^n = P(x) = \prod_{i=1}^{2g+1} (x - x_i)^{d_i}$$

where the x_i are real numbers and the d_i are integers. This amounts to saying that the surface is a cyclically branched cover over the Riemann sphere punctured on the real axes.

Let a meromorphic 1-form ω on X be given by

$$\omega = T(x) \frac{dx}{y}$$

with some rational function $T(x)$ such that

$$F(x) = T(x)P(x)$$

is a polynomial of some degree d. We have in mind $\omega = Gdh$. Here the the rational function is

$$T(x) = \frac{1}{x^2 - a^2}.$$

The goal is to compute (numerically) the periods of this form ω.

From cohomological considerations it follows that we are able to write

$$\frac{F(x)}{y^{n+1}} dx - \frac{A(x)}{y} dx = d\frac{R(x)}{y} \tag{13}$$

with new polynomials A and R. So instead of $\int_\gamma \frac{F(x)}{y^{n+1}} dx$ we can now compute $\int_\gamma \frac{A(x)}{y} dx$, which can be done along a real line segment $x_i x_{i+1}$. However, the task remains to find $A(x)$ explicitly.

By differentiating the Riemann surface equation

$$y^n = P \Rightarrow ny^{n-1}dy = P'dx \Rightarrow dy = \frac{P'}{ny^{n-1}}dx$$

we get that for an arbitrary function f on X

$$
\begin{aligned}
y\frac{df(x)}{y} &= y\frac{yf'dx - fdy}{y^2} \\
&= f'dx - \frac{1}{n}\frac{P'}{P}fdx
\end{aligned}
$$

Hence (1) is equivalent to

$$
\begin{aligned}
F - y^n A &= y^n(R' - \tfrac{1}{n}\tfrac{P'}{P}R) \\
\Leftrightarrow \qquad F - P(A + R') &+ \tfrac{1}{n}P'R = 0
\end{aligned}
$$

This equation allows one to find the coefficients of the polynomials A and R by solving a symbolic linear system of equations, provided certain technical conditions on the degree of P are satisfied (which we don't care about).

Solving this symbolic system is still not an obvious task, if the rank of the system is large (say 10). One can get around this as follows:

Solving (13) for A gives

$$A = \frac{nF + P'R}{nP} - R' \tag{14}$$

As A will be a polynomial, we have to find R with $\deg R \leq 2g$ such that

$$nF + P'R \equiv 0 \pmod{P} \tag{15}$$

To solve this equation, we first solve

$$P'Q \equiv 1 \pmod{P}$$

That is we seek polynomials Q and S such that

$$QP' = SP + 1$$

At the $2g + 1$ places x_i where P vanishes, we deduce that necessarily

$$Q(x_i) = \frac{1}{P'(x_i)}$$

69

so that we can write down a candidate for Q using Lagrange interpolation:

$$
\begin{aligned}
Q(x) &= \sum_{i=1}^{2g+1} \prod_{j \neq i} \frac{x - x_j}{x_i - x_j} \frac{1}{P'(x_i)} \\
&= \sum_{i=1}^{2g+1} \frac{P(x)}{x - x_i} \lim_{x \to x_i} \frac{x - x_i}{P(x)} \frac{1}{P'(x_i)} \\
&= P(x) \sum_{i=1}^{2g+1} \frac{1}{(x - x_i) P'(x_i)^2}
\end{aligned}
$$

Using this, we get R from (15) as

$$
R = -nQF \pmod{P}
$$

and this allows to compute A by (14).

Because our F will always share many zeroes with P, it is much faster to compute R directly by Lagrange interpolation using the fact that

$$
R(x_i) = -n \frac{F(x_i)}{P'(x_i)}
$$

All this is quite easy to implement. For a variation, it is conceivable that there are other kinds of replacements if one looks only at the singularities which actually cause trouble for the cycle over which one wants to integrate.

Finally, we give the results of the computation in the simplest case:

Example 7.5 (The CHM_1 surface) Here we have for Gdh

$$
\begin{aligned}
P(x) &= x^2(x^2 - 1)(x^2 - a^2) \\
F(x) &= x^2(x^2 - 1) \\
R(x) &= -2 \frac{x(x^2 - 1)}{a^2(a^2 - 1)} \\
A(x) &= \frac{3x^2 - a^2}{a^2(a^2 - 1)}
\end{aligned}
$$

References

[Cos82]   C. Costa. *Imersöes minimas en* $\mathbb{R}^3$ *de gênero un e curvatura total finita.* PhD thesis, IMPA, Rio de Janeiro, Brasil, 1982.

[Cos84]   C. Costa. Example of a complete minimal immersion in $\mathbb{R}^3$ of genus one and three embedded ends. *Bull. Soc. Bras. Mat.*, 15:47–54, 1984.

[DHKW92] U. Dierkes, S. Hildebrandt, A. Küster, and O. Wohlrab. *Minimal Surfaces I.* Grundlehren der mathematischen Wissenschaften 296. Springer-Verlag, 1992.

[FK80]   H. M. Farkas and I. Kra. *Riemann Surfaces.* Number 72 in Graduate texts in mathematics. Springer-Verlag, 1980.

[Gun66]   R. C. Gunning. *Lectures on Riemann Surfaces.* Princeton University Press, Princeton, N.J., 1966.

[HK97]   D. Hoffman and H. Karcher. Complete embedded minimal surfaces of finite total curvature. In *Encyclopedia of Mathematics*, pages 5–93, 1997. R. Osserman, editor, Springer Verlag.

[HKW93]   D. Hoffman, H. Karcher, and F. Wei. The genus one helicoid and the minimal surfaces that led to its discovery. In *Global Analysis and Modern Mathematics.* Publish or Perish Press, 1993. K. Uhlenbeck, editor, p. 119–170.

[JS66]   H. Jenkins and J. Serrin. Variational problems of minimal surface type, ii. boundary value problems for the minimal surface equation. *Arch. Rational Mech. Anal.*, 21:321–342, 1965/66.

[Kar88]   H. Karcher. Embedded minimal surfaces derived from Scherk's examples. *Manuscripta Math.*, 62:83–114, 1988.

[Kar89]   H. Karcher. Construction of minimal surfaces. *Surveys in Geometry*, pages 1–96, 1989. University of Tokyo, 1989, and Lecture Notes No. 12, SFB256, Bonn, 1989.

[LHI98]   H. Lazard-Holly and W.H. Meeks III. Classification of doubly-periodic minimal surfaces of genus zero. preprint, 1998.

[Lop92]   F. J. Lopez. The classification of complete minimal surfaces with total curvature greater than -12π. *Trans. Amer. Math. Soc.*, 334(1):49–74, 1992.

[LR91]   F. J. Lopez and A. Ros. On embedded complete minimal surfaces of genus zero. *Journal of Differential Geometry*, 33(1):293–300, 1991.

[MPR98]   W.H. Meeks, J. Pérez, and A. Ros. Uniqueness of the riemann minimal examples. *Invent. math.*, 131:107–132, 1998.

[Neh52]   Z. Nehari. *Conformal Mapping.* Dover, New York, 1952.

[Oss86]   R. Osserman. *A Survey of Minimal Surfaces.* Dover Publications, New York, 2nd edition, 1986.

[Sat96]   K. Sato. Existence proof of one-ended minimal surfaces with finite total curvature. *Tohoku Math. J.*, 48:229–246, 1996.

[Sch83]   R. Schoen. Uniqueness, symmetry, and embeddedness of minimal surfaces. *Journal of Differential Geometry*, 18:791–809, 1983.

[Ste96]   M. Steffens. Doppelt periodische minimalflächen. Diplom thesis, 1996.

[Web99]   M. Weber. Period quotient maps of meromorphic 1-forms and minimal surfaces on tori. preprint Bonn, 1999.

[Web00]   M. Weber. On singly periodic minimal surfaces invariant under a translation. *Manuscripta Mathematica*, 101:125–142, 2000.

[WW98]   M. Weber and M. Wolf. Minimal surfaces of least total curvature and moduli spaces of plane polygonal arcs. *Geom. and Funct. Anal.*, 8:1129–1170, 1998.